GIMA
Geographical Information Management and Applications

MSc. thesis:

CHARACTERISATION OF WETLAND TYPES USING SENTINEL-1 RADAR TIME SERIES DATA

March 1st, 2019

Author:	Bart Slagter
Email address:	bartslagter94@gmail.com
Supervisors:	dr. Nandika Tsendbazar (WUR)
	dr. Johannes Reiche (WUR)
Responsible professor:	dr. ir. Ron van Lammeren (WUR)

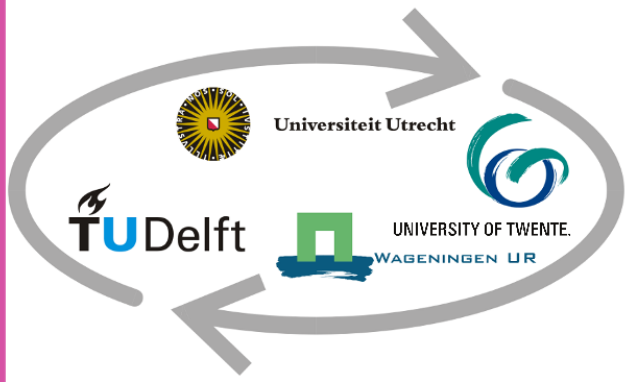

Preface

This thesis was written as part of the MSc. programme Geographical Information Management & Applications. It comprises a detailed documentation of a five-month research, conducted from September 2018 until March 2019.

Special thanks go to my supervisors Nandika Tsendbazar and Johannes Reiche from Wageningen University & Research, who introduced me to this challenging topic and guided me during the research process.

Bart Slagter,
March 1st, 2019.

Summary

During the last decades, wetlands have been determined as one of the most valuable ecosystems on Earth. Despite their importance for both humanity and nature, they are also one of the most rapidly degrading land cover types. In order to implement and evaluate effective policy for wetland preservation, large-scale monitoring and characterisation of wetlands is needed. The use of satellite-based remote sensing techniques has proven its use for this purpose. However, wetland mapping and characterisation by using remote sensing is challenging.

The recently launched Sentinel-1 satellites acquire radar images with a relatively high spatial and temporal resolution, using C-band dual-polarimetric (VV/VH) sensors. This new data-rich information source provides a unique opportunity for more accurate wetland monitoring from space. In this research, the temporally dense Sentinel-1 radar time series data was applied for wetland characterisation and its use was assessed. The combination of Sentinel-1 and Sentinel-2 data was also applied to additionally assess the use of Sentinel-1 when combined with optical satellite data.

In order to assess the use of Sentinel-1 data for wetland characterisation, four different machine learning classifications were done in the St. Lucia wetlands in South Africa, based on a classification scheme with three levels of wetland characterisation: (1) general wetland delineation, (2) the classification of wetland vegetation types and (3) the classification of surface water dynamics. The sole use of Sentinel-1 and the combined use of Sentinel-1 and Sentinel-2 were both applied. As the C-band radar system aboard Sentinel-1 was expected to have limited capabilities in mapping high-vegetated wetlands, an additional set of classifications was done excluding these high-vegetated wetlands. Each classification was done in a Monte Carlo simulation of 100 Random Forests in order to obtain reliable results.

It was found that Sentinel-1 radar data is useful for mapping low- to medium-vegetated wetlands. However, it is incapable of distinguishing high-vegetated wetlands from upland forests. The combined use of Sentinel-1 and Sentinel-2 delivered significant accuracy improvements compared with the sole use of Sentinel-1. The value of Sentinel-2 was especially observed for general wetland delineation.

Table of Contents

1 Introduction

1.1 Background

1.1.1 Wetlands and their Degradation

During the last decades, wetlands have been determined as one of the most valuable ecosystems on Earth. As of 2018, 168 countries are signed under the Ramsar Convention, which is a global environmental agreement developed in 1971, aimed at the conservation and wise use of wetlands (Ramsar Secretariat, 2016). Some important functions of wetlands are water storage, water purification, shoreline protection, processing of carbon and other nutrients, food security, and the support of a large biodiversity in plants and animals (Millennium Ecosystem Assessment, 2005; Ramsar Secretariat, 2016). In addition, these functions of wetlands are essential in achieving the Sustainable Development Goals (SDGs) as stated by the United Nations (Ramsar Secretariat, 2018). It is assumed, that at least 11 of the 17 main SDGs are supported by the functions of wetlands.

Despite the importance of wetlands for both humanity and nature, they are also one of the most rapidly degrading land cover types. The Millennium Ecosystem Assessment (2005) has estimated that approximately 50% of all global wetlands has been lost during the 20th century. Extensive irrigation practices, extraction of groundwater, and the change of wetlands into urban or agricultural lands are the main causes. It is also stated that wetlands are degrading at a rate faster than any other ecosystem. To prevent further loss of wetlands and implement and evaluate policy for wetland preservation, it is important to monitor the total extent of wetlands and also to characterise different wetland types. Nowadays, many attempts have already been done to map and characterise wetlands on a local, regional or global scale and several methods have been used.

1.1.2 Monitoring of Wetlands

On-site monitoring of wetlands is highly informative, but is also expensive (Gallant, 2015). In addition, many wetlands are in remote and inaccessible locations. Therefore, field monitoring is only possible for a small subset of global wetlands. Monitoring on a larger scale is needed to provide regional or global information about wetlands. In order to obtain such large scale information, satellite-based Earth observation is the most effective mean (Mahdavi et al., 2018; Ozesmi & Bauer, 2002). Satellite-based Earth observation is widely used for automated land cover classifications in general, where the combination of satellite images and machine learning methods, such as Support Vector Machines, Decision Trees and especially Random Forests, has proven its use (Keshtkar et al., 2017; Rodriguez-Galiano et al., 2012).

Two main techniques for satellite-based Earth observation are optical and radar remote sensing. Optical sensors usually operate in the visual and infrared portions of the electromagnetic

spectrum and sense the solar reflectance of the Earth surface. Optical remote sensing has the advantage that many spectral bands of reflectance can be distinguished, providing a variety of information about land cover and land use. Although optical remote sensing has been used for wetland mapping in many ways, it has often been found to be insufficient for this purpose (Bourgeau-Chavez et al., 2009; Ozesmi & Bauer, 2002), mainly because it is can only acquire useful data during the day and in cloud-free weather. Therefore, considerable effort has also been put in the use of radar remote sensing for wetland mapping. Radar sensors operate in the microwave range of the electromagnetic spectrum and transmit pulses sideways in order to sense backscattering. Radar is capable of providing different characteristics of the Earth surface than optical sensors are. It can be highly informative for wetland detection, because radar backscattering is sensitive to surface properties like moisture, roughness and especially the occurrence of water bodies (Henderson & Lewis, 2008). Radar remote sensing has another advantage that it can operate in all weather conditions during day and night, because it is not dependent on sunlight as illumination source and clouds are easily penetrated by radar pulses. Therefore, radar remote sensing can achieve a higher temporal density in useful images than optical remote sensing. This is an advantage for mapping wetlands that are highly dynamic in terms of flooding. Especially because many wetland areas are located in tropical or coastal regions that experience periods of persistent cloud cover (Clint Slatton et al., 2008; Li et al., 2006; Novresiandi & Nagasawa, 2015), radar is the most efficient mean for mapping. Longer wavelength radar systems are also capable of penetrating vegetation to a certain extent. As water bodies can occur at subcanopy level, this is a valuable quality of radar for wetland detection in highly vegetated areas, such as swamp- or mangrove forests (Ozesmi & Bauer, 2002). A disadvantage of radar is that there is a limited availability of open data (Guo et al., 2017). Also, pre-processing of radar data can be time-consuming.

In the past, mapping and characterising wetlands by using remote sensing has had several limitations. An important factor is that wetlands are difficult to delineate from other land cover classes. Wetlands are not unified by a common land cover type or vegetation type, but only share the characteristic ‘presence of water’ (Gallant, 2015). Besides delineating wetlands from other land cover classes, the characterisation of different wetland types is also challenging. Although different wetland types have their distinctive characteristics, they also share some ecological characteristics with each other (Bunn et al., 1997), and with other non-wetland land cover types (Henderson & Lewis, 2008). Wetlands can also be highly dynamic in terms of their flooding levels, resulting in different spectral or backscattering information during time (Gallant, 2015). For this reason, satellites need a short revisit time in order to accurately map areas that experience temporary flood events. Moreover, when flooding is present under a forest’s canopy its detection is difficult or even impossible when using shorter radar wavelengths or optical data (Rosenqvist et al., 2007). Because of the low spatial resolution of most satellite images it is also difficult to identify smaller wetland areas. In the past, this has led to underestimations of the total extent of wetlands (Ozesmi & Bauer, 2002). For accurate mapping, a relatively high spatial resolution is needed. Although the use of optical data has been

determined to be inferior to radar data for wetland mapping, optical data is often used as a complement besides radar to improve mapping accuracies (Henderson & Lewis, 2008; Ozesmi & Bauer, 2002).

Another difficulty for large-scale wetland characterisation, is the difference in wetland definitions (Amler et al., 2015), which has resulted in the use of different wetland classification schemes around the world (Mahdavi et al., 2018). Some of the wetland classification schemes are highly detailed. Although these complex classification schemes are useful for on-site characterisation, they are less suitable for remote sensing-based classifications, as such level of detail is often beyond what satellite sensors can deliver. Therefore, remote sensing-based classifications often use higher-level characteristics, where vegetation types and dynamics in surface water are determined as key characteristics of wetlands (Keddy, 2010; Mitsch & Gosselink, 2006; Tiner, 1999).

1.1.3 Sentinel-1 Radar

As part of the Copernicus programme of the European Space Agency (ESA), the Sentinel-1 radar mission provides a unique opportunity for more accurate wetland monitoring from space. The first Sentinel-1 satellite was launched in 2014. Currently, there are two Sentinel-1 satellites in orbit, which carry a C-band Synthetic Aperture Radar (SAR) system, acquiring data in single- and dual-polarimetric modes (European Space Agency, 2018). The ESA provides Sentinel-1 radar images free of charge. The Level-1 Ground Range Detected (GRD) products have a relatively high spatial resolution (10 metres in pixel size) and temporal resolution (6 days revisit time at the equator). The combination of these relatively high resolutions is a good specification when compared with other radar satellites, such as ERS1/2 and Envisat (Li et al., 2016). Many studies have verified that a higher spatial resolution can improve the accuracy of wetland monitoring (Guo et al., 2017). The higher temporal resolution can provide a better accuracy in order to deal with the dynamic flood levels that occur in wetlands (Cazals et al., 2016). Therefore, the Sentinel-1 radar images are promising for better results in wetland mapping.

1.2 Problem Statement

With Sentinel-1 available now, for the first time radar data is provided free of charge in high spatial and temporal resolutions. The data gives the opportunity for new insights in wetland mapping methods. Regarding this newly available data, several studies have already been done for wetland mapping and characterisation. However, the focus in these studies has been mainly on single-date analyses (Chatziantoniou et al., 2017; Kaplan & Avdan, 2018a; Whyte et al., 2018), specific types of wetlands (Cazals et al., 2016; Kaplan & Avdan, 2018b; Mleczko & Mróz, 2018; Mróz et al., 2016; Tsyganskaya et al., 2018), specific wetland characteristics (Huang et al., 2017; Muro et al., 2016; Tian et al., 2017; Xing et al., 2018), or used a non-globally applicable approach (Mahdianpari et al., 2018). It is not yet clear what value the high-resolution and temporally dense data has for accurate wetland delineation, and for detailed

mapping of the two most important wetland characteristics, defined as: vegetation types and surface water dynamics.

Research aimed at the potential of Sentinel-1 data for mapping and characterising wetlands in multiple levels is necessary to exploit the new data-rich information source and assess its value. First, it is needed to assess to what extent the dense Sentinel-1 time series data is capable of delineating wetlands from non-wetlands in general. Wetlands are here defined in their broadest sense, as all areas that can be classified between upland and permanent water. There have been no studies yet that exploit the use of Sentinel-1 time series data for this single purpose. Second, the use of Sentinel-1 time series data for characterising differences in wetland vegetation types needs to be studied, as this has been a challenging aspect for C-band radar in the past. Third, the use of Sentinel-1 time series data for characterising wetlands in terms of their surface water dynamics needs to be studied, especially in combination with their vegetation types. Recent studies have looked at many wetland characteristics separately, but no assessments have been done to map the complex systems of wetlands in a comprehensive way using Sentinel-1 time series data. It is needed to assess how the complexity of wetlands influences the accuracy of wetland classifications using this new data. A multi-level approach using Sentinel-1 time series data is necessary to investigate this.

As optical data has proven its use as a complement besides radar for wetland characterisation, a valuable addition for an assessment of Sentinel-1 time series data is to test its combined use with optical data from Sentinel-2. A comparison between the sole use of Sentinel-1 time series data and its combined use with Sentinel-2 can place the assessment of Sentinel-1 more in perspective. This comparison can also indicate the value of using optical data besides the Sentinel-1 time series data.

1.3 Research Objective

As stated, the use of Sentinel-1 data for wetland mapping and characterisation needs to be studied. Therefore, the main objective of this research is to assess the use of temporally dense and high spatial resolution Sentinel-1 radar time series data for mapping and characterising different wetland types. The research objective will be reached by answering the following research questions:

1. How accurate can wetlands be mapped within different levels of characterisation, using Sentinel-1 time series data?
2. What is the accuracy improvement for wetland characterisation when combining Sentinel-1 time series data with optical data from Sentinel-2?
3. How and to what extent are the accuracies of the produced maps affected by the complexities in wetland characteristics?

The first research question is aimed at an assessment of the use of Sentinel-1 data for different levels of wetland characterisation, considering the most important wetland characteristics. The second question is aimed at assessing the combined use of Sentinel-1 with optical data from Sentinel-2. The third research question is aimed at the evaluation of the results obtained in the first two questions. Here, the focus lies on the complexities, such as vegetation flooding and water dynamicity, that make wetlands a challenging land cover type to map.

1.4 Societal and Scientific Relevance

Scientific relevance

Many remote sensing-related studies have been done with the purpose of wetland mapping and characterisation. Different radar wavelengths, polarisations and combinations with other data sources have been used. The freely available Sentinel-1 data and its resolutions, polarimetry and wavelength, are a new unique combination of sensor characteristics. The capabilities of this radar satellite system need to be researched in the domain of wetland mapping, in order to assess the value of this new system in relation to other wetland mapping methods.

Societal relevance

The seriousness of concerns about the rapid degradation of wetlands is underlined by the global recognition of wetland importance by the Ramsar Convention. Also, many of the recently defined SDGs of the United Nations are supported by the functions of wetlands. In order to implement and evaluate effective policy for wetland preservation, large-scale monitoring and characterisation of wetlands is needed. During the last decades, radar remote sensing has proven its use here, although mapping has been challenging due to wetlands being highly dynamic and complex as a land cover type. The new Sentinel-1 data, which is free of charge and has a high spatial and temporal resolution, provides the opportunity for better monitoring of wetlands. The use and value of this data needs to be researched, in order to use the data effectively in the future and make it of assistance in wetland preservation.

1.5 Reading Guide

The following chapters give an outline of the research that has been conducted towards the use of Sentinel-1 radar time series data for wetland mapping and characterisation. Chapter 2 gives an overview of remote sensing-based methods for wetland mapping. The use of both radar and optical remote sensing are shortly discussed within this domain. Also, several past studies related to wetland mapping using Sentinel-1 are described. Chapter 3 gives an overview of the methodology used for this research. The study area, used data, pre-processing steps, reference data, classification methods and validation methods are outlined here. In Chapter 4, the results are presented per classification level. In Chapter 5, the main results are discussed and some limitations in the research methodology are pointed out. Chapter 6, the concluding chapter, gives a brief overview of the main findings. Also, recommendations for further research are done here.

2 Theory

In this chapter, the theoretical background of this research is outlined. Chapter 2.1 discusses the theory and classification schemes for wetland delineation and characterisation. In Chapter 2.2 the use of radar- and optical remote sensing for wetland mapping is discussed. Here, the use of Sentinel-1 data and past wetland research using this data is outlined more in detail. Chapter 2.3 gives an overview of the concepts discussed.

2.1 Wetland Delineation and Characterisation

The broadest wetland definition is *"A land transitional between terrestrial and aquatic systems"*, as defined by Cowardin et al. (1979). During the last decades, many other definitions of wetlands have been established. As a result, a severe challenge for wetland research is that a uniform wetland definition within land cover classifications does not exist (Amler et al., 2015), which makes delineation of wetlands difficult.

Besides general wetland delineation, the characterisation of different wetland types is even more complex, as there are also no uniform definitions for distinct wetland classes. This has resulted in several different wetland classifications schemes, which have been established and acknowledged on national and global scales (Tiner et al., 2015). Two of the best-known and most comprehensive examples are the classifications used by Ramsar (Ramsar Secretariat, 2009) and the US Fish & Wildlife Service (as designed by Cowardin et al., 1979). These multi-level classification schemes distinguish respectively 40 and 55 wetland types and are highly detailed. However, this also makes them less suitable for remote sensing-based classifications, where such level of detail is often beyond what satellite sensors can deliver. In existing remote sensing-based wetland classifications that do have a high level of detail, it is often found that they are limited to classifications within one certain wetland type, such as swamps, marshes or peatlands (Rosenqvist et al., 2007), or to classifying one certain characteristic, such as water depth, water periodicity, quality of water, vegetation types or soil types (Semeniuk & Semeniuk, 1997).

For characterising wetlands with remotely sensed data in a more comprehensive way, several classification methods have already been designed to distinguish wetland types. A well-known example of a such a comprehensive classification is the distinction of wetlands in bogs, fens, marshes and swamps. The Canadian Wetland Classification System (CWCS) (National Wetlands Working Group, 1997) is a well-known description of such a classification and is widely used due to its overarching geographical application (Mahdavi et al., 2018). However, a wetland being classified in one of these four types is often determined by higher level characteristics, of which some are easier to classify using remote sensing, such as vegetation types and surface water dynamics. Also, when using machine learning-based classifications,

acquiring training data with limited resources is much easier for vegetation types and surface water dynamics than for the classes used in the CWCS, which often require on-site observations.

According to Tiner (1999), many remote sensing-based wetland characterisations have there basis in classifying vegetation types. However, he stated that the focus on vegetation types alone is insufficient and characterisations of hydrology and hydric soils are also necessary to comprehensively characterise wetlands. This is confirmed by Mitsch & Gosselink (2006) who stated that the three core components of wetlands are soil type, vegetation type and dynamics in water levels. Keddy (2010) stated that the dynamics in water levels is the most important characteristic in wetlands, because this affects many other processes within a wetland, such as the development of the other two main characteristics: soil- and vegetation types. In earlier studies aimed at remote sensing-based characterisation of wetlands, radar data has shown its capabilites especially for mapping vegetation types and surface water dynamics (Henderson & Lewis, 2008). The characterisation of soil types often requires on-site measurements.

For the characterisation of these two important wetland characteristics, several examples exist, using radar or including radar data in multi-sensor analyses. Classifications of wetlands based on surface water dynamics have been done by i.a. Bourgeau-Chavez et al. (2005), Moser et al. (2016), Rosenqvist et al. (2002), Schlaffer et al. (2016) and Ward et al. (2014). They used radar data in time series analyses to classify wetlands in terms of their flooding levels. More comprehensive classifications of wetlands, in terms of both surface water dynamics and vegetation types, have been done by i.a. Hess & Melack (1994), Hess et al. (2003), Martinez & Le Toan (2007) and Töyrä & Pietroniro (2005). In these studies, wetland vegetation types are often characterised in ordinal categories, like herbaceous, shrubby and forested wetland. The use of the U.S. National Vegetation Classification Standard (NVCS) (Federal Geographic Data Committee, 1997), which is a basic ordinal vegetation classification scheme with several distinct classes, has proven its usefulness for delineating different vegetation classes in wetlands.

2.2 Remote Sensing-Based Wetland Mapping

2.2.1 Wetland Mapping Using Radar Remote Sensing

Radar remote sensing has been widely used for wetland mapping. The main advantages of radar for this purpose are that it is very sensitive to water, it is not limited by blockage of clouds, it is not dependent on daylight as illumination source, and it is capable of penetrating vegetation to a certain extent. Two important characteristics of a radar sensor are its wavelength and polarimetry. These concepts and their relation to wetland mapping are briefly outlined below.

Wavelength

Radar sensors transmit and receive pulses within a certain wavelength band (Figure 1). The most common wavelength spectra used in remote sensing-based wetland characterisations are

C-band (3.75 – 7.5 cm) and L-band (15 – 30 cm) (Henderson & Lewis, 2008). In general, the larger the wavelength, the more penetration in Earth surface objects is possible. These penetration capabilities of radar systems are especially of importance for wetland mapping, because this enables the detection of water bodies at subcanopy level in high-vegetated wetlands, such as swamp- or mangrove forests. This detection is possible due to a scatter mechanism called 'double-bounce scattering'. In vegetated wetlands, this occurs when radar waves penetrate vegetation canopy and thereafter double bounce between a water surface and tree trunks or wooded vegetation (Hess et al., 1990; Richards et al., 1987). This results in a high backscattering value.

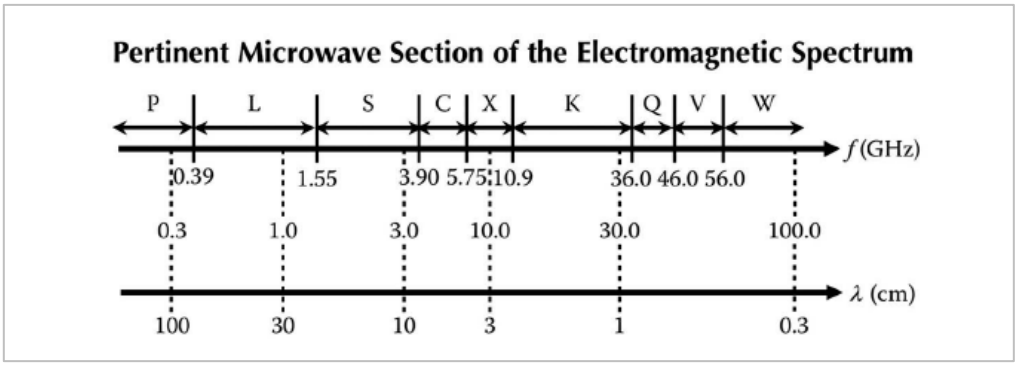

Figure 1: Radar bands and their corresponding frequency (f) and wavelength (λ) (Lee & Pottier, 2009).

Double-bounce scattering in forested wetlands is especially well observed using longer-wavelength radar systems, such as L-band or P-band, because these systems are capable of full penetration in most forest's canopies (Hess et al., 1995; Wang et al., 1995). Therefore, for wetland characterisation in forested wetlands, the use of L-band has demonstrated to be superior to C-band. Another advantage of L-band radar is that specular reflection from water surfaces is better observed in wavy conditions, making L-band better capable of distinguishing water and upland. After the launch of ESA's BIOMASS satellite in 2021, which will carry a P-band radar system aboard (European Space Agency, 2019), the use of an even longer wavelength can be explored for wetland mapping from space. Wang et al. (1995) already acknowledged that P-band systems can outperform L-band for subcanopy flood detection in the most densely forested wetlands.

Despite the fact that L-band is favoured for mapping flooded forests, Wang et al. (1995) also noted that C-band had a modest potential for mapping subcanopy flooding. Many subsequent studies aimed at mapping flooded forests using C-band systems (e.g. ERS, Envisat, Radarsat) obtained varying results (Henderson & Lewis, 2008). The ability of C-band to penetrate a forest's canopy and observe small amounts of double-bounce scattering is dependent on a variety of factors working in tandem (e.g. radar polarimetry, radar incidence angle, canopy

closure, canopy volume, tree species) (Kasischke & Bourgeau-Chavez, 1997; Townsend, 2002; Wang et al., 1995). Although mapping high-vegetated wetlands is sometimes possible using C-band, its capacities can best be used for mapping lower-vegetated wetlands, such as herbaceous or shrubby wetlands, where C-band is favoured over L-band (Henderson & Lewis, 2008). For mapping such wetlands, less vegetation penetration is needed.

Polarimetry

A second important characteristic of a radar sensor is its polarimetry. This determines whether pulses are transmitted and received either in horizontal (H) or vertical (V) orientation at the sensor (Figure 2). This distinguishes three key polarisation modes, stated below (the first letter denotes transmission and the second letter denotes receive):

- Single-polarimetric: operating in a single mode of transmit and receive orientation (HH, HV, VH or VV).
- Dual-polarimetric: transmitting in a single orientation and receiving in both (HH and HV or VV and VH) or transmitting and receiving in the same orientations (HH and VV).
- Quad-polarimetric: transmitting and receiving in all four combinations of orientation (HH, HV, VH and VV).

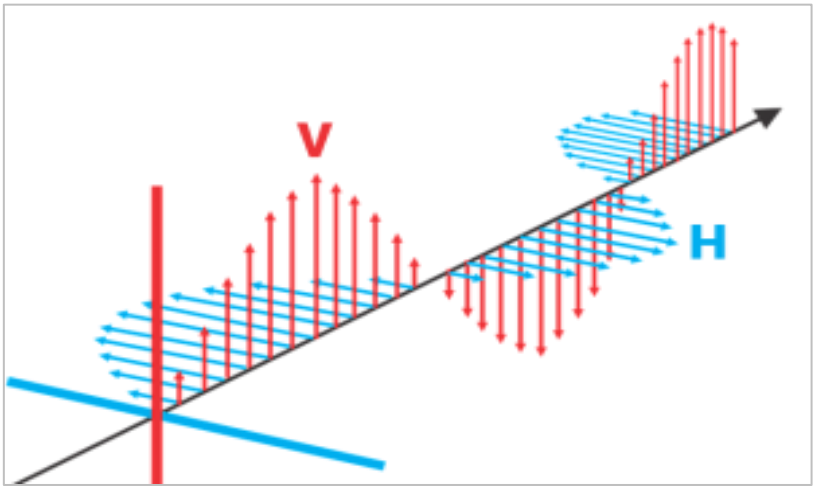

Figure 2: Radar polarimetry. The orientation of transmit and receive can be either vertical (red) or horizontal (blue) (www.gisgeography.com).

For wetland characterisations using radar, HH-polarised images have shown the best results, mainly because double-bounce scattering from flooded vegetation and specular reflection from water bodies are best observed in this mode (Baghdadi et al., 2001; Brisco et al., 2011). Although HH mode is better at observing double-bounce scattering during subcanopy flooding, VV mode has also shown moderate capabilities to do this under the right circumstances (Townsend, 2002). The use of a cross-polarised (VH or HV) component besides a co-polarised

(VV or HH) component is useful, because cross-polarisation performs well at measuring the occurrence of vegetation, due to volume scattering in leaves and twigs (Kuga et al., 1990).

Because the different modes of radar waves interact differently with objects on the Earth surface, each of the four (or three, as HV and VH do not deliver major differences) possible modes delivers different information. Although single-polarimetric radar can be useful to detect calm water bodies, it is not very effective for more complex wetland characterisations, because the information delivered in single mode is not comprehensive enough (Mahdavi et al., 2018). The maximum number of backscattering values (four) is acquired in quad-polarimetric mode. This mode delivers the most comprehensive information for land cover classifications. Still, the use of a dual-polarimetric mode – which delivers only half the backscattering values compared with the quad-polarimetric mode – can have its benefits. An important advantage of dual-polarimetric radar is that it can acquire data with a wider swath width and can therefore cover larger areas of Earth surface in a certain time (Ainsworth et al., 2009).

The most important disadvantage of a dual-polarimetric mode is the impossibility to make use of advanced polarimetric decompositions, which demand quad-polarimetric data. The use of polarimetric decompositions (e.g. the Cloude-Pottier, Touzi, Freeman-Durden or Yamaguchi decompositions) has proven its great potential for wetland mapping (Furtado et al., 2016; Mahdianpari et al., 2017). However, data coverage provided by quad-polarimetric systems is very limited.

The use of dual-polarimetric radar still gives the possibility to extract indices or ratios from the separate polarisations. Often, a ratio between two polarisations is taken (e.g. VV/VH or HH/HV). Also, the normalized difference between two polarisations is regularly used as a variable for wetland characterisation (Guo et al., 2017).

2.2.2 Wetland Mapping Using Optical Remote Sensing

Optical remote sensing has been used for general land cover classifications in many ways. The ability of optical remote sensing to split surface reflectance into multiple wavelength bands makes it a valuable technique to detect different processes on the Earth surface. However, the limitations of optical remote sensing, being in need of daylight and being unable to penetrate clouds and vegetation, make it less useful for wetland mapping specifically. Especially in temporally dense time series analyses, which are preferred over single-image analyses, the hindrance of cloud cover is a large disadvantage in the use of optical data. In the past, multiple studies have reported that the sole use of optical sensors is insufficient for accurate wetland mapping (Bourgeau-Chavez et al., 2009; Ozesmi & Bauer, 2002). Especially in highly dynamic wetland areas that are subject to persistence cloud-cover, the use of optical data is limited.

Still, the information provided by optical sensors can be complementary to radar data (Henderson & Lewis, 2008; Ozesmi & Bauer, 2002). Multispectral sensors can be used to

measure reflections in certain wavelength bands in the visible and infrared portions of the electromagnetic spectrum. Reflectance values from these bands can be used either as individual measures, or as ratios or indices of multiple bands combined. Related to wetland characterisation, the use of red-edge reflectance or near-infrared (NIR) reflectance as single bands can be useful (Mahdavi et al., 2018). When compared to the use of single bands, the strength of indices lies in their ratioing aspect, which reduces many forms of multiplicative noise (e.g. illumination differences, cloud shadows, atmospheric attenuation, certain topographic variations) present in multiple bands and throughout multiple dates (Chen et al., 2002; Huete et al., 2002). Several indices related to vegetation and water can be of assistance for wetland characterisation. These are briefly outlined below.

Vegetation index

The Normalised Difference Vegetation Index (NDVI), which is the most widely used vegetation index, is a measure for the normalised difference between near-infrared (NIR) and red reflectance (Kriegler et al., 1969). As live vegetation has a high reflectance in the NIR portion of the electromagnetic spectrum and a low reflectance in the red, it is an often-used indicator for the amount of photosynthetically active biomass. NDVI can discriminate vegetation and non-vegetation, as well as wetlands and non-wetlands. For wetland characterisations, NDVI can also be of value for classifying different types of vegetation.

Water indices

The Normalised Difference Water Index (NDWI) is a measure for the normalised difference between the green and NIR reflectance (McFeeters, 1996). The approach of the NDWI is very similar to the NDVI, but in this case the index is an indicator for the occurrence of water bodies. Therefore, the NDWI is a valuable measure for wetland characterisation. Xu (2006) reported that the NDWI as proposed by McFeeters (1996) showed better results for water body detection when the short-wave infrared (SWIR) band is used instead of the NIR band. As a result, he developed the Modified NDWI (MNDWI), which is the normalised difference between the green and SWIR reflectance.

Other wetness-related indices are the Normalised Difference Moisture Index (NDMI) for the normalised difference in NIR and SWIR (Gao, 1996), and the Normalised Difference Pond Index ($NDPI_o$; o denotes 'optical', to indicate the difference with the NDPI related to radar data) for the normalised difference in SWIR and green reflectance. However, relative to the (M)NDWI, these indices are not frequently used for wetland characterisations. The NDMI is aimed at measuring moisture in vegetation and is less useful for water body detection (Gao, 1996). The $NDPI_o$ is no more than a negative from the MNDWI, because it uses the same spectral bands, but in the opposite order of extraction. Therefore, using both MNDWI and $NDPI_o$ has no added value in machine learning-based land cover classifications.

2.2.3 Studies Applying Sentinel-1 Data for Wetland Mapping

Data acquisition of the Sentinel-1 satellites is done with a C-band (with an exact wavelength of 5.55 cm) dual-polarimetric SAR system. Being dual-polarimetric means in this case that data is acquired in VV and VH mode over land, except in the polar regions, where HH and HV mode are used (European Space Agency, 2018).

As the Sentinel-1 images are currently providing openly available data with better spatial and temporal resolutions, they are an interesting new data source in the domain of radar-based wetland mapping. Regarding this newly available data, several studies have been done for wetland mapping and characterisation. These past studies have focussed mainly on single-date approaches, specific wetland types, specific wetland characteristics or a non-globally applicable use. These studies, of which many also incorporated optical data, are briefly summarised below.

Single-date approaches

Chatziantoniou et al. (2017), Kaplan & Avdan (2018a) and Whyte et al. (2018) integrated images from Sentinel-1 and Sentinel-2 for wetland mapping. Although they obtained a high accuracy for wetland classifications, their analyses were based on images from a single date, thus neglecting the multi-temporal aspect. All authors recommended the use of a multi-temporal approach for further research. As stated by Gallant (2015), the use of multi-temporal images is important for accurate wetland characterisation, due to the dynamics of surface water in these areas.

Multi-temporal approaches aimed at specific wetland types

Several studies have applied a multi-temporal approach for wetland mapping with Sentinel-1 data. Cazals et al. (2016) used Sentinel-1 data in a multi-temporal approach to analyse the hydrological dynamics of a marsh wetland. They reported the great potential of dense Sentinel-1 time series data for seasonal flood mapping. Multi-temporal approaches have also been adopted by Mroz et al. (2016) and Mleczko & Mróz (2018), who tested Sentinel-1 for mapping herbaceous wetlands. They concluded that the use of Sentinel-1 data obtained relatively inaccurate results for this purpose. Tsyganskaya et al. (2018) researched the use of Sentinel-1 time series data to detect temporary flooded vegetation within wetlands and proved the value of Sentinel-1 here. Kaplan & Avdan (2018b) used Sentinel-1 time series data, combined with optical and thermal data, to classify wetlands as swamps, bogs or sedimentary bogs. They studied and confirmed several correlations between radar, optical and thermal variables. Many of these studies have illustrated the great potential of Sentinel-1 time series data, especially for monitoring variations in seasonal floods with a high temporal frequency. However, these studies have focussed on specific wetland types. Therefore, their generic and global applicability for wetland characterisation in general is discussable.

Multi-temporal approaches aimed at specific wetland characteristics

Several multi-temporal approaches with Sentinel-1 data to map specific characteristics of wetlands have also been done. Huang et al. (2017), Tian et al., (2017) and Xing et al. (2018) used Sentinel-1 time series to classify wetlands based on flood frequencies. They proposed successful methods to indicate surface water dynamics in wetlands, based on per-image classifications of water and non-water. Muro et al. (2016) used Sentinel-1 time series data to detect short term wetland changes in two European Ramsar sites. Their research was also mainly focused on analysing one characteristic, namely surface water dynamics.

Multi-temporal approach not globally applicable

Mahdianpari et al. (2018) used Sentinel-1 time series data, combined with optical data from Sentinel-2, to classify wetlands according to the CWCS. Their study area, being in a near-polar region, gave them the advantage of using both VV/VH and HH/HV modes of Sentinel-1. A main finding in their study was that the combined use of both Sentinel-1 and optical data significantly improved the results. Unfortunately, the use of both dual-polarimetric Sentinel-1 modes is not globally applicable.

2.3 Conceptual Framework

Figure 3 shows an overview of the concepts discussed in this chapter. It is a graphical display of the relevant domains within both land cover classifications and remote sensing. Together they comprise the potential use of Sentinel-1 for wetland characterisation.

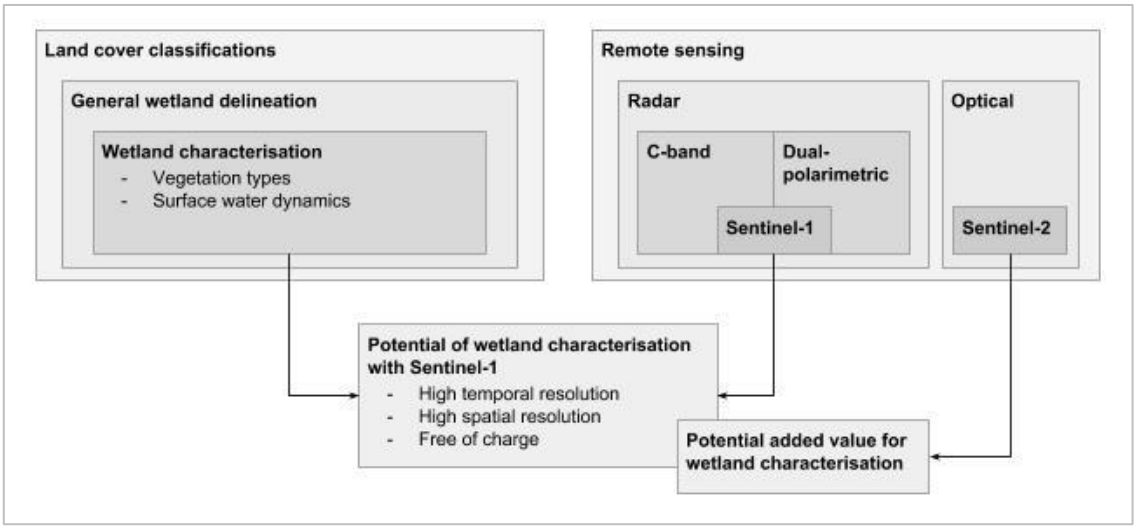

Figure 3: Conceptual framework for wetland characterisation.

3 Methodology

This chapter describes the methodology of this research, of which a detailed overview can be found in Figure 4. In Chapter 3.1 the used study area is described. In Chapter 3.2 the data acquisition and pre-processing steps of the Sentinel-1 and Sentinel-2 data are outlined. Chapter 3.3 describes the used wetland classification scheme, based on three different levels. In Chapter 3.4 the used reference data and the acquisition of training- and validation samples is outlined. Chapter 3.5 describes the classification methods. In Chapter 3.6 the validation methods are discussed.

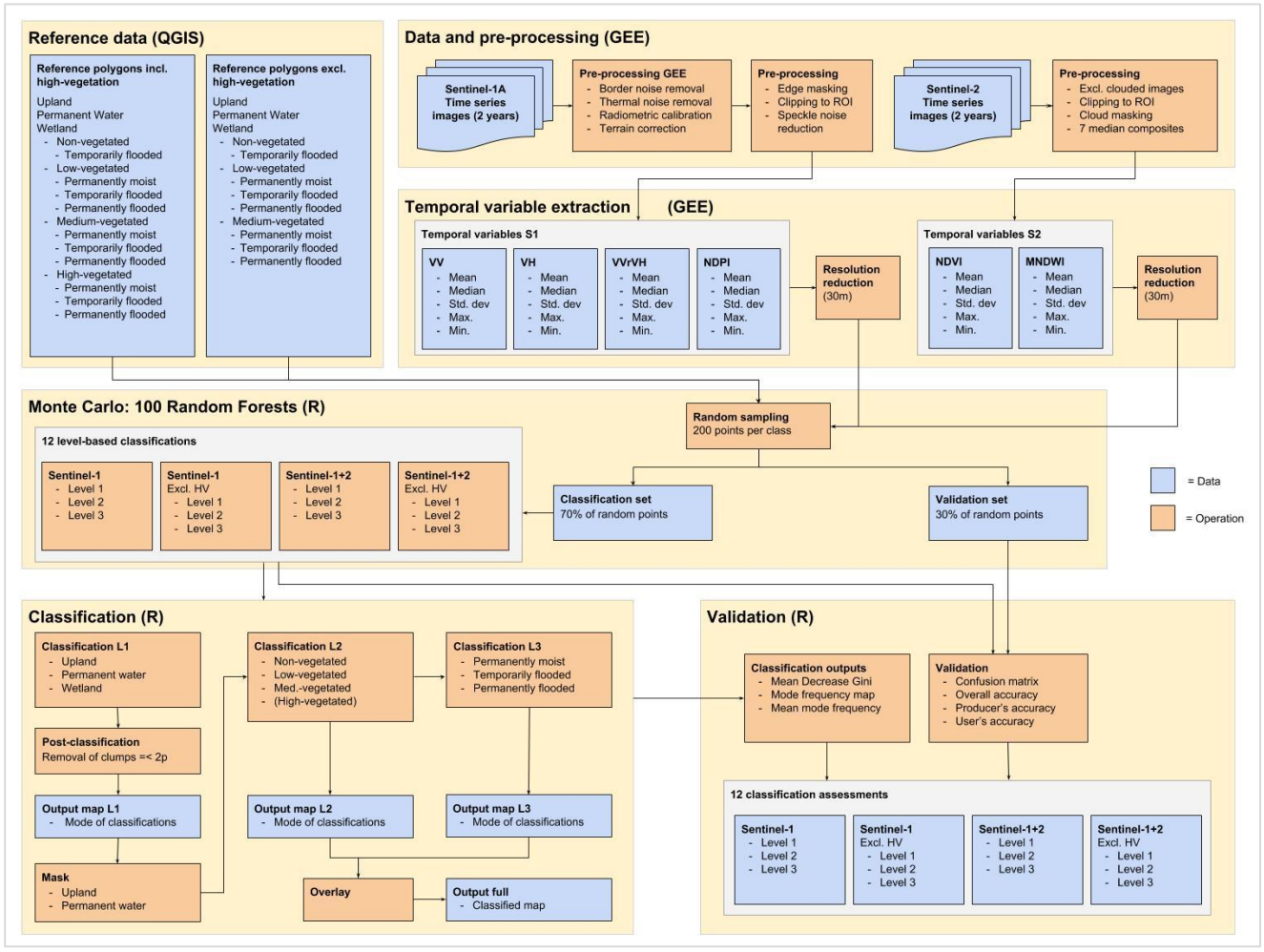

Figure 4: Workflow for data acquisition, pre-processing, classification and validation.

3.1 Study Area

The characterisation of wetlands, by using Sentinel-1 data and the combination of Sentinel-1 and Sentinel-2 data, was applied in the St. Lucia wetlands (also known as the iSimangaliso

wetlands) in South Africa. The St. Lucia wetlands are a UNESCO World Heritage site and an official Ramsar site. The used study area is a smaller region within the actual site as defined by Ramsar (Figure 5). This sub area was chosen in order to reduce the processing time for the classifications. The selected region was determined to be suitable as a testing area, because it has a variety of wetlands types. All wetland types as defined in the classification scheme in Chapter 3.3 occur within this area. The size of the area is approximately 640 km², which corresponds to 6.4 million pixels of full resolution Sentinel-1 and Sentinel-2 data per image band.

A side note for this specific wetland area is that it has been subject to a restoration process. The goal of this restoration is to enlarge the water inflow into the area. During the 21st century, the St. Lucia wetlands had been subject to severe droughts, which reached their peak during February 2016 (iSimangaliso Wetland Park, 2017). Since the start of the earliest summer rainfall in October 2016 the water levels have been more stable. The restoration project had been a contributory cause in this.

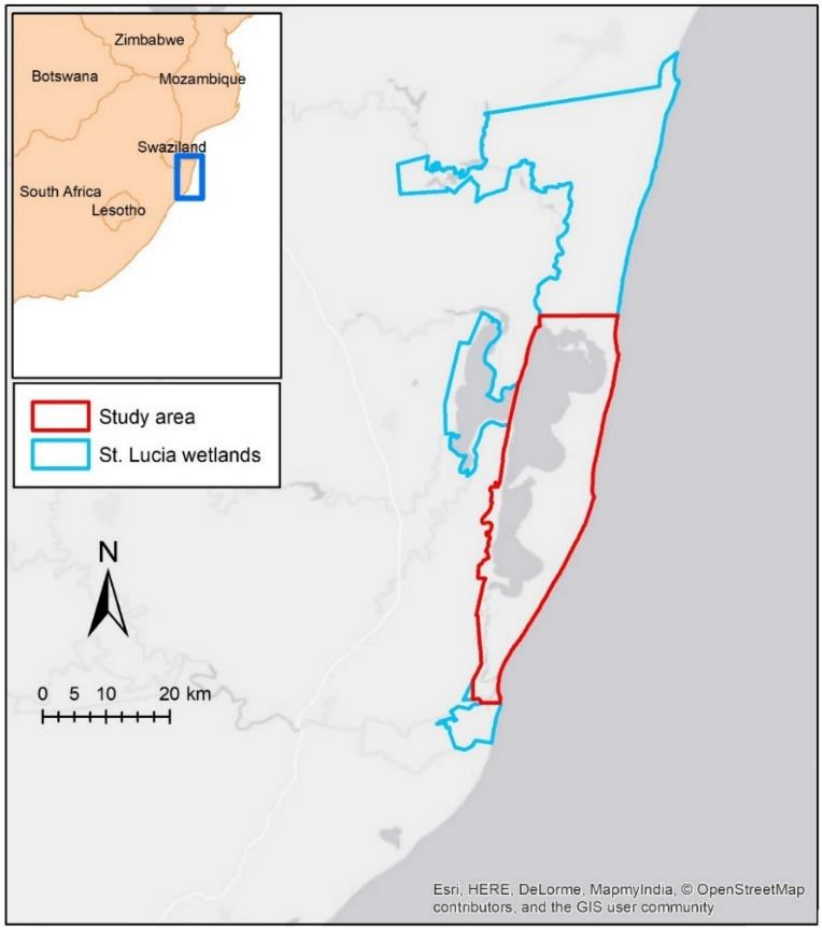

Figure 5: Map of the study area. The study area is a sub-area of official St. Lucia wetland boundaries as defined by Ramsar.

3.2 Data

3.2.1 Sentinel-1 Data and Pre-processing

The Sentinel-1 data product was acquired and pre-processed in Google Earth Engine (GEE) (Google, 2018a), using its JavaScript-based code editor. The Sentinel-1 Level-1 data provided within GEE is Ground Range Detected (GRD) and has a 10-metre resolution. The instrument mode is Inferometric Wide Swath (IW). In the study area images are only acquired in ascending mode. This means that the side-looking orientation of the sensor is always the same, namely west to east. GEE was chosen as a tool for pre-processing, because of its capacities to process large amounts of data within a cloud-based platform.

The entire study area is covered by a single Sentinel-1 image footprint, so mosaicking of multiple images was not needed (Figure 6). As stated in Chapter 3.1, the study area had been subject to droughts until late 2016. Therefore, it was chosen to select images from after this period for the analyses, from October 2016 until October 2018. This two-year period covers two cycles of wet seasons (usually around January – March) and dry seasons (usually around May – September), starting and ending in the transition between these extremes. This selection resulted in a total of 61 Sentinel-1A images, with a 12-day revisit time (Table 1). The full temporal resolution of 6 days revisit time could not be used, because Sentinel-1B images were not available in GEE. Still, the revisit time of 12 days was considered to be dense enough for accurate classifications.

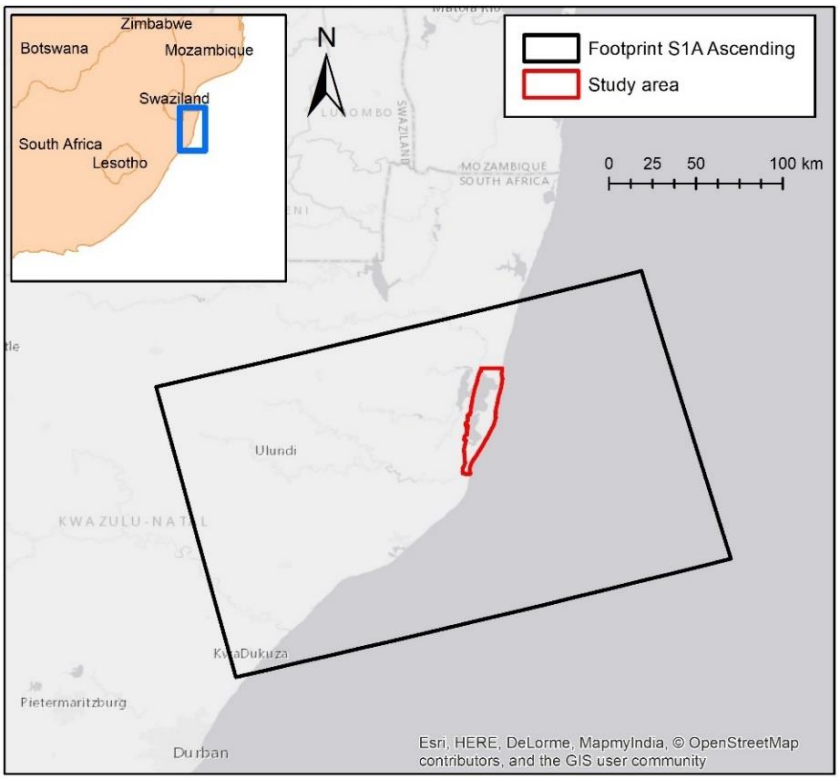

Figure 6: The image footprint of the Sentinel-1A images in ascending mode.

Table 1: Acquisition dates of the 61 Sentinel-1A GRD images used for the analyses.

	2016	2017	2018
January		8th, 20th	3rd, 15th, 27th
February	*Peak drought*	1st, 13th, 25th	8th, 20th
March		9th, 21st	4th, 16th, 28th
April		2nd, 14th, 26th	9th, 21st
May		8th, 20th	3rd, 15th, 27th
June		1st, 13th, 25th	8th, 20th
July		7th, 19th, 31st	2nd, 14th, 26th
August		12th, 24th	17th, 19th, 31st
September	*Drought ending*	5th, 17th, 29th	12th, 24th
October	4th, 16th, 28th	11th, 23rd	
November	9th, 21st	4th, 16th, 28th	
December	3rd, 15th, 27th	10th, 22nd	

Within GEE, the acquired Sentinel-1 images were already pre-processed using the following steps (Google, 2018b):

- GRD border noise removal: Removes low intensity noise and invalid data on scene edges.
- Thermal noise removal: Removes additive noise in sub-swaths to help reduce discontinuities between sub-swaths for scenes in multi-swath acquisition modes.
- Radiometric calibration: Computes backscatter intensity using sensor calibration parameters in the GRD metadata.
- Terrain correction (orthorectification): Converts data from ground range geometry, which does not take terrain into account, to sigma nought values using the SRTM 30-metre DEM.

Besides these pre-processing steps done for the data product in GEE, several additional steps were taken. First, all areas with extremely high and low incidence angles were excluded. This resulted in masking out the edges of all images. The images were then clipped to the extent of the study area as displayed in Figure 5. Speckle noise reduction was applied with a 5 x 5 pixel median filter. This filter is a moving window that takes the median value of a 5 x 5 pixel area and assigns this value to the window's centred cell. Apart from coastal dunes at the shores, the study area is relatively flat. Therefore, no radiometric terrain flattening was applied. A pre-processed radar image of the entire study area can be found in Appendix 1.

The VV and VH backscattering values were used for the wetland classifications, complemented with the ratio between VV and VH (VVrVH) and the Normalized Difference Polarisation Index for VV and VH (NDPI). An overview of these variables derived from the images can be found in Table 2. The used temporal statistics for these values were mean, median, standard deviation, maximum and minimum, which were calculated over the two-year period. An overview of the used temporal variables can be found in Table 3.

Table 2: Overview of derived variables from the 61 Sentinel-1 images.

Value	Description	Equation
VV	Backscattering value for vertical transmit and vertical receive.	*NA*
VH	Backscattering value for vertical transmit and horizontal receive.	*NA*
VVrVH	A ratio to indicate the VV backscattering relative to the VH backscattering.	$VVrVH = \frac{VV}{VH}$
NDPI	A ratio to indicate the normalized difference between the VV and VH backscattering.	$NDPI = \frac{VV - VH}{VV + VH}$

Table 3: Overview of used Sentinel-1 temporal variables.

VV	VH	VVrVH	NDPI
Mean	Mean	Mean	Mean
Median	Median	Median	Median
Standard deviation	Standard deviation	Standard deviation	Standard deviation
Maximum	Maximum	Maximum	Maximum
Minimum	Minimum	Minimum	Minimum

In total, this resulted in a stacked image with 20 values per pixel, representing the temporal statistics of Sentinel-1 data for the two-year period. It was assumed that that noise by outliers, which would especially affect the maximum and minimum, were reduced by the median filter in the pre-processing steps. After the calculation of these temporal variables the resolution was reduced to 30 metres, by using the mean pixel values of a 3 x 3 window. This was done because processing is much faster in a coarser resolution. A 30-metre resolution was considered to be high enough for detailed wetland mapping.

3.2.2 Sentinel-2 Data and Pre-processing

Sentinel-2 data from the same two-year period was used as additional data for the classifications of wetlands. The Sentinel-2 satellites are equipped with a multispectral sensor, distinguishing 13 spectral bands in the visible, NIR and SWIR portions of the electromagnetic spectrum (Figure 7). The first satellite (Sentinel-2A) was launched in June 2015 and the second (Sentinel-2B) in March 2017 (European Space Agency, 2018). This meant that the used data within the two-year period obtained a higher temporal density after March 2017.

The Sentinel-2 data was also acquired and pre-processed in GEE, where the images are provided as a Level-1C product representing Top of Atmosphere (TOA) reflectance. Images are provided with a 10-metre resolution for the shorter wavelengths and a 20- or 60-metre resolution for longer wavelengths or narrower bandwidths.

Figure 7: Graphic display of spectral band measurements of the multispectral sensor aboard the Sentinel-2 satellites (European Space Agency, 2015).

In order to remove the most clouded images from the time series, only images with a cloud-cover less than 40% were selected. Mosaicking was not needed, because the Level-1C data in GEE is provided in tiles and not as separate images. After filtering the most clouded images, image tiles remained from 160 distinct days for the study area. Masking of remaining clouds and cirrus was done for all these images by using threshold values for band 2 (for the removal of dense clouds) and band 10 (for the removal of cirrus clouds). A pre-processed optical image of the entire study area can be found in Appendix 2.

Within the total period of two years, quarterly median composites were produced. This means that for all the images within a three-month period, the median pixel values were taken. The use of these median composites is preferred over using the single images, because disturbances (especially due to inaccuracies in cloud masking) that highly affect the temporal variables can be neutralised. The first quarter (October, November and December 2016) was removed from the analyses, because persistent cloud cover during this period restricted the use of a proper median composite here. The final result comprised seven median composites of Sentinel-2 images. An overview of the used median composites is given in Figure 8.

	2016			2017										2018								
	Oct	Nov	Dec	Jan	Feb	Mar	Apr	May	Jun	Jul	Aug	Sep	Oct	Nov	Dec	Jan	Feb	Mar	Apr	May	Jun	Jul	Aug	Sep
Median composites	Excluded						Composite 2						Composite 4						Composite 6					
				Composite 1						Composite 3						Composite 5						Composite 7		

Figure 8: Overview of used time frames for the seven quarterly median composites of Sentinel-2.

Two indices were calculated for each quarterly median composite. These were the NDVI for vegetation detection and the MNDWI for water body detection. An overview of these calculated variables can be found in Table 4. The used temporal statistics for these values were the same as for Sentinel-1, namely mean, median, standard deviation, maximum and minimum, which were calculated from the seven median composites within the two-year period. An overview of the used temporal variables can be found in Table 5.

Table 4: Overview of derived variables from the seven Sentinel-2 median composites.

Value	Description	Equation
NDVI	A measure to indicate the occurrence of vegetation based on the normalised difference in NIR (band 8) and red (band 4) reflectance.	$NDVI = \frac{NIR - Red}{NIR + Red}$
MNDWI	A measure to indicate the occurrence of water bodies based on the normalised difference in green (band 3) and SWIR (band 11) reflectance.	$MNDWI = \frac{Green - SWIR}{Green + SWIR}$

Table 5: Overview of used Sentinel-2 temporal variables.

NDVI	MNDWI
Mean	Mean
Median	Median
Standard deviation	Standard deviation
Maximum	Maximum
Minimum	Minimum

In total, this resulted in a stacked image with 10 values per pixel, representing the temporal statistics of Sentinel-2 data for the two-year period. After the calculation of these temporal variables, the resolution was also reduced to 30 metres, by using the mean pixel values of a 3 x 3 window. For the classification of wetlands by using both the Sentinel-1 variables and the Sentinel-2 variables, the images were overlaid into a stacked image of 30 variables in total.

3.3 Classification Scheme

3.3.1 Levels and Classes

For the comprehensive characterisation of wetlands, a classification scheme was designed based on three levels. These levels were defined conform the most important wetland characteristics as described in Chapter 2.1: vegetation types and surface water dynamics. Prior to these two levels, one classification level was defined to delineate wetlands from uplands and permanent water. In the subsequent classification levels four vegetation types and three

types of surface water dynamics were distinguished. An outline of the classification and the distinct classes within the levels is given below:

- Level 1 classification: General wetland delineation
    - Permanent water
    - Upland
    - Wetland
- Level 2 classification: Classifying vegetation types
    - Non-vegetated wetland
    - Low-vegetated wetland
    - Medium-vegetated wetland
    - High-vegetated wetland
- Level 3 classification: Classifying surface water dynamics
    - Permanently moist wetland
    - Temporarily flooded wetland
    - Permanently flooded wetland

A graphical overview of this classification scheme can be found in Figure 9. The red dotted line in the figure indicates the classes for high-vegetated wetlands. Sentinel-1, being a C-band radar system, has limited capabilities to detect these high-vegetated wetlands. It was expected that including these wetlands in the classifications would disturb the results to a certain extent. For example: misclassifications in Level 1 due to high confusion between upland forests and high-vegetated wetlands would force the classification of many uplands into meaningless subclasses in Level 2 and Level 3. This would lead to confusion in Level 2 and Level 3, that could be traced back to errors that actually occurred in Level 1. In order to avoid such confusions when evaluating the use of Sentinel-1 data for wetland characterisation, two different sets of classifications were done: one with high-vegetated wetlands included and one with high-vegetated wetlands excluded. It was expected that the latter would reduce confusion in Level 2 and Level 3 caused by errors in Level 1.

In total, this classification scheme leads to ten wetland classes and two non-wetland classes. Excluding the high-vegetation classes means that seven wetland classes are distinguished. The combinations ‘permanently moist, non-vegetated wetland’ and ‘permanently flooded, non-vegetated wetland’ do not exist within this scheme. The first combination would be a highly unlikely phenomenon. The second combination defines the same as the Level 1 class ‘permanent water’ and can therefore not be defined as a wetland. As a result, a non-vegetated wetland is always defined as ‘temporarily flooded’ within this scheme.

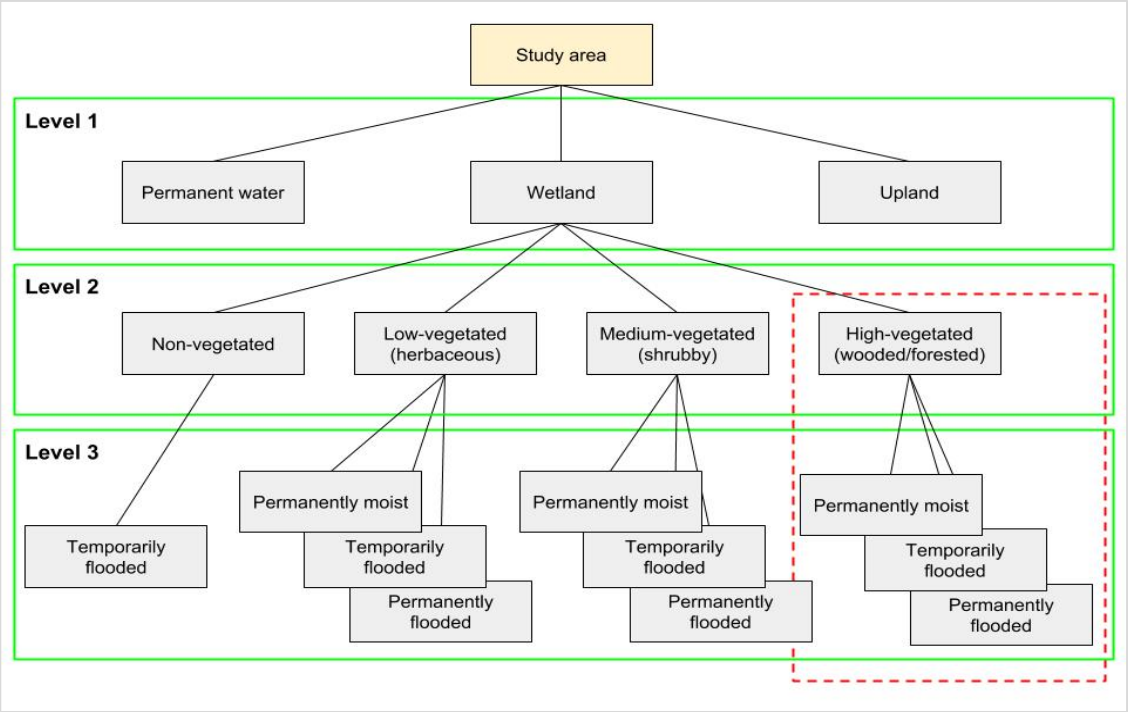

Figure 9: Classification scheme.

3.3.2 Class Definitions

In order to classify the different wetland types, definitions were established for each class. These definitions were used to select suitable reference samples for the classifications, which is further described in Chapter 3.4. The definitions in Level 1 are simple: Upland comprises all terrestrial land cover types (e.g. forests, grasslands, urban areas, agricultural land, bare soil) and permanent water comprises all areas that are covered with water at least 80% of time. Wetlands are all areas in between these definitions of upland and permanent water. The definitions of classes as defined in Level 2 and Level 3 are outlined more detailed in Table 6 and Table 7. The definitions for vegetation types were derived from the classes defined by the NVCS (Federal Geographic Data Committee, 1997). Examples of each wetland class displayed in high-resolution aerial images can be found in Figure 10.

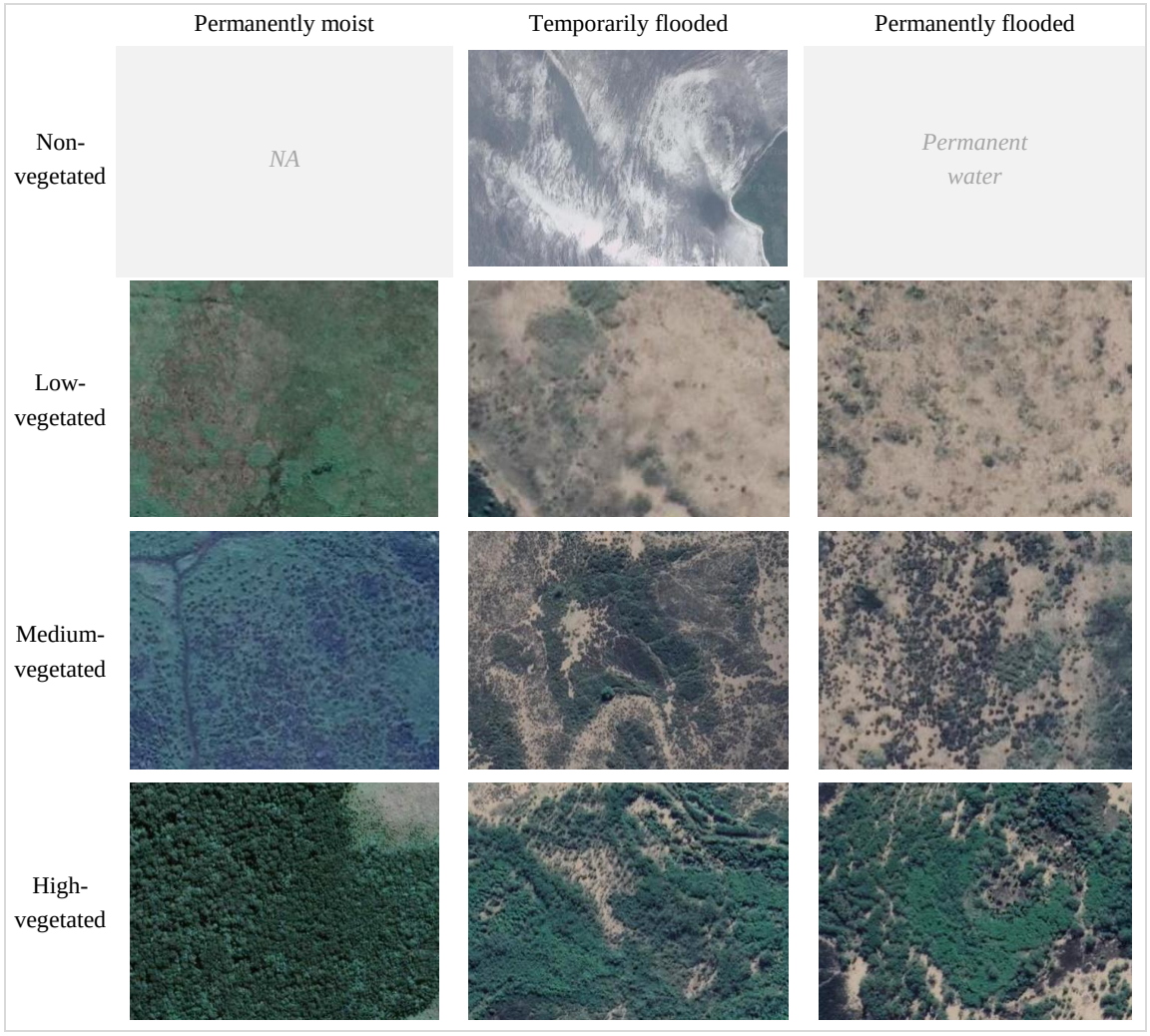

Figure 10: Aerial images of examples of wetland classes. Images in the class 'temporarily flooded' were taken during a flood event. The brownish colours indicate the occurrence of water (Google, 2018c).

Table 6: Definitions used for Level 2: vegetation types.

Defined class	Description	NVCS description	NVCS thresholds
Non-vegetated	Wetlands with no vegetation, such as mudflats.	Non-vegetated or sparsely vegetated.	<10% vegetation cover.
Low-vegetated (herbaceous)	Wetlands with herbaceous vegetation, such as low-vegetated marshes.	Vascular plants without significant woody tissue above the ground.	<0.5 metre in height. <25% shrub- or forested cover.
Medium-vegetated (shrubby)	Wetlands with shrubby vegetation, such as higher vegetated marshes.	Woody plants that exhibit several erect, spreading, or prostate stems that give a bushy appearance.	>0.5 metre in height. <5 metre in height. >25% shrubby cover.
High-vegetated (wooded/forested)	Wetlands covered by trees, such as swamp- or mangrove forests.	Woody plants, usually with a single main stem and a definite crown.	>5 metre in height. >25% forested cover.

Table 7: Definitions used for Level 3: surface water dynamics.

Defined class	Description	Thresholds
Permanently moist	Wetlands that have a constant occurrence of low amounts of water, but do not experience severe floods.	Flooded: <20% of time.
Temporarily flooded	Wetlands that are subject to severe flood events with high amounts of water.	Flooded: >20% of time and <80% of time.
Permanently flooded	Wetlands that are constantly or nearly constantly flooded with high amounts of water.	Flooded: >80% of time.

3.4 Reference Data

3.4.1 Data Sources

As stated in Chapter 3.3, the classification of wetlands was based on three levels. In order to acquire reference samples from the study area to use as training- and validation data, several land cover datasets, local studies, data analyses and aerial or satellite images were used. These are described in Table 8, Table 9, Table 10 and Table 11 respectively. More specific, the classification level where the source was used for the collection of reference samples is stated under 'Level'.

Table 8: Description of land cover datasets used as input for the selection of reference samples.

Dataset	Description	Author/reference	Level
Global Surface Water Dataset	30-metre resolution map of global dynamics in surface water from 1984-2015.	Pekel et al. (2016)	1, 3
Tropical & Subtropical Wetland Distribution	231-metre resolution classification of wetland types in tropical and sub-tropical regions.	Gumbricht et al. (2017)	1, 2
South African Land Cover Dataset	30-metre resolution general land cover classification of South Africa	GeoTerraImage (2015)	1, 2
NFEPA Wetlands	Vector map with classification of wetland types in South Africa.	(Council for Scientific and Industrial Research, 2011a)	1, 2
NFEPA Wetland Vegetation	Vector map with classification of wetland vegetation types in South Africa.	(Council for Scientific and Industrial Research, 2011b)	2
Vegetation Map of South Africa, Lesotho and Swaziland	Vector map with classification of general vegetation types in South Africa.	Rutherford et al. (2007)	2

Table 9: Description of local studies used as input for the selection of reference samples.

Author/reference	Description	Level
Clulow et al. (2013)	Land cover classification of the Mfabeni mire site within the St. Lucia wetlands.	1, 2
Lück-Vogel et al. (2016)	Detailed land cover classification in the surroundings of the St. Lucia village.	1, 2
Maseko et al. (2017)	Land cover classification in the entire area of the St. Lucia wetlands.	1
Whyte et al. (2018)	Land cover classification in the entire area of the St. Lucia wetlands.	1, 2

Table 10: Description of datasets used for analyses as input for the selection of reference samples.

Dataset	Description	Author/reference	Level
Shuttle Radar Topography Mission (SRTM)	30-metre resolution global digital elevation model. Used as an extra check for wetland and upland delineation.	Farr et al. (2007)	1
Sentinel-1 SAR Ground Range Detection	10-metre resolution C-band SAR images. Temporal signatures for VV and VH backscattering were used as an indicator for surface water dynamics.	European Space Agency (2017a)	3
Sentinel-2 Level 1C	10- and 20-metre resolution multispectral images. Derived variables for reference sample collection were (M)NDWI and NDVI. Temporal signatures for (M)NDWI were used as an indicator for surface water dynamics and NDVI measures were used as an indicator for wetland vegetation types.	European Space Agency (2017b)	2, 3
PALSAR-2 Global 25m Resolution Mosaic 2017	25-metre resolution HH and HV L-band SAR images from the PALSAR-2 sensor aboard the ALOS-2 satellite. The provided images were taken in 2017 and were used to indicate the occurrence of high-vegetated wetlands.	Shimada et al. (2014)	1, 2
Planet satellite images	3-metre resolution global composition of satellite images with a high temporal resolution. Images from different dates can be viewed. Used as an indicator for surface water dynamics.	Planet (2018)	1, 3

Table 11: Description of aerial images used as input for the selection of reference samples.

Dataset	Description	Author/reference	Level
Google Earth images	High-resolution global composition of aerial images and satellite images in different scales and from different dates.	Google (2018c)	1, 2, 3
Microsoft Bing Maps images	High-resolution global composition of aerial images and satellite images in different scales.	(Microsoft Bing Maps, 2018)	1, 2
South African aerial photography	0.5-metre resolution aerial photography of South Africa.	National Geospatial Information (2018)	1, 2

3.4.2 Training- and Validation Points

All datasets described in Table 8, Table 9 and Table 11, were loaded and geographically overlaid into QGIS (QGIS Development Team, 2018). The datasets from Table 10 were loaded within GEE, except for the Planet satellite images, which were used within the platform Planet Explorer (Planet, 2018).

Visual interpretation and – to a lesser extent – threshold values were used to acquire suitable reference samples. Reference samples were initially acquired by drawing polygons. These reference sample polygons were drawn based on a reasonable certainty that could be derived from the sources described in Table 8, Table 9, Table 10 and Table 11. Polygons were only drawn for areas where multiple sources pointed out the occurrence of a wetland area, a certain wetland vegetation class or a certain type of surface water dynamics. In other words, multiple sources needed to have an overlap in a certain area, for that area to be determined as a reference sample polygon.

The reference sample polygons were labelled for the wetland classes they represented in each level of classification, resulting in three labels per reference sample polygon. These polygons were used as stratification to generate the random sample points, which were subsequently used as training and validation for the automated wetland classifications. The use of polygons as stratification for generating random sample points ensured that all classes as defined in Chapter 3.3.1 – also spatially underrepresented classes such as non-vegetated wetland and permanently flooded wetland – were represented within the reference samples.

The random sample points were generated with a minimum distance constraint of 45 metres, which is slightly larger than the diagonal distance of the 30 x 30 metre pixels in the pre-processed Sentinel-1 and Sentinel-2 images. This constraint was needed to avoid the placement of multiple random sample points within the same pixel, which would eventually result in multiple representations of the same training- or validation sample.

3.5 Classification Method

3.5.1 Classification Algorithm

All classifications were done within R (R Core Team, 2018). R was preferred over GEE, because machine learning-based classification methods are easier applied within R. Random Forest (Breiman, 2001) was used as method for the wetland classifications. Random Forest is a machine learning method that can be used for supervised classifications. It is based on the automatic construction of multiple decision trees, where each tree takes a random subset of input variables and training objects for classifications. For a final decision of an object's classification, each tree gets one 'vote' in the end result. Random Forests have proven their use for classifications with large amounts of data in satellite images (Wurm et al., 2017) and

also for radar-based classifications specifically (Zhou et al., 2018). Random Forests outperform standard classification methods for land cover, because they can handle the large differentiation within land cover classes and noise data can be neutralised (Rodriguez-Galiano et al., 2012).

The Random Forest classifier uses training data in order to construct the decision trees. The temporal variables from the Sentinel-1 and Sentinel-2 data, as described in Chapter 3.2.1 and 3.2.2, were used as input variables. These variables were extracted from the underlying pixel values in the images with 200 random sample points per class. The classifications were done with 70% of the random sample points used as training data. The remaining 30% were used for validation (described in Chapter 3.6). This means that all classifications were done with a 70% subset of 600 random sample points, except the classifications in Level 2 that include high-vegetated areas. In these classifications the four vegetation types were classified with a 70% subset of 800 random sample points in total.

The split in training- and validation points was done randomly before each classification. The number of trees in each Random Forest classification was set to 128, which is determined to be the optimal number in the consideration between accuracy and processing speed for Random Forests (Oshiro et al., 2012). To limit the tree depth and prevent the trees from overfitting, the minimum node size was set to 5. It was chosen to keep these parameters of the Random Forests the same for all classifications in all levels, in order to obtain comparable results.

For each classification, two outputs were produced: A classified map and a Mean Decrease in Gini (MDG) for all used variables. The MDG is a measure of how pure a variable can be split at a node in a Random Forest. This measure indicates the importance of the distinct variables used for the classifications. Another commonly used variable importance measure is the Mean Decrease in Accuracy (MDA). The use of this measure as an additional result was ignored, because of highly comparable variable rankings for both the MDG and MDA. An important note for the use of such variable importance measures, is that they tend to be biased towards correlated variables (Nicodemus, 2011; Strobl et al., 2008). As many of the temporal statistics obtained from Sentinel-1 and Sentinel-2 are highly correlated, the interpretation of the MDGs should be done cautiously.

In order to obtain a robust result and neutralise the randomness in the classifications, a Monte Carlo approach was used to generate the final outputs. This means that all classifications were run 100 times. The 100 output maps from the classifications were overlaid and the majority pixel values were taken to produce the final output maps. The final MDG was obtained by taking the mean MDGs per variable from these 100 classifications. Although the mean MDGs were generated from the classification, their interpretation was mainly part of the evaluation.

Additional outputs from the 100 classifications were a mode frequency map and a mean mode frequency per class. As these outputs were mainly interpreted as part of the validation, they are further explained in Chapter 3.6.

3.5.2 Classifications

The designed classification scheme and the used satellite images resulted in 12 possible classifications. These 12 possibilities are the result of the different combinations of input data and classification levels. An overview is given in Table 12.

Table 12: Overview of all classification combinations, addressed with distinct abbreviations.

	Including high-vegetation		Excluding high-vegetation	
	Sentinel-1	**Sentinel-1 and Sentinel-2**	**Sentinel-1**	**Sentinel-1 and Sentinel-2**
Level 1	*S1L1*	*S1S2L1*	*S1L1-HV*	*S1S2L1-HV*
Level 2	*S1L2*	*S1S2L2*	*S1L2-HV*	*S1S2L2-HV*
Level 3	*S1L3*	*S1S2L3*	*S1L3-HV*	*S1S2L3-HV*

In the Level 1 classifications, wetlands were distinguished from uplands and permanent water. The results of these classifications were post-classified to reduce a so-called 'salt-and-pepper' effect. This means that all isolated pixel clumps that consisted of only one or two pixels were removed from the output maps. The adjacency of pixels was determined in eight directions, which is the so-called 'queen's adjacency'. The values of these isolated pixels were replaced by the majority pixel value of its direct neighbours in a 3 x 3 window.

The post-classified output maps from these Level 1 classifications were used as an input for the Level 2 and Level 3 classifications, where upland and permanent water were masked out. The non-masked areas – the wetlands – were then further classified for their vegetation types (Level 2) and surface water dynamics (Level 3). The output maps from all levels were overlaid, in order to obtain a final output: a full classification of all considered wetland types. These final output maps included 12 classes for the classifications with high-vegetated areas included and 9 classes for classifications with high-vegetated areas excluded (Figure 11).

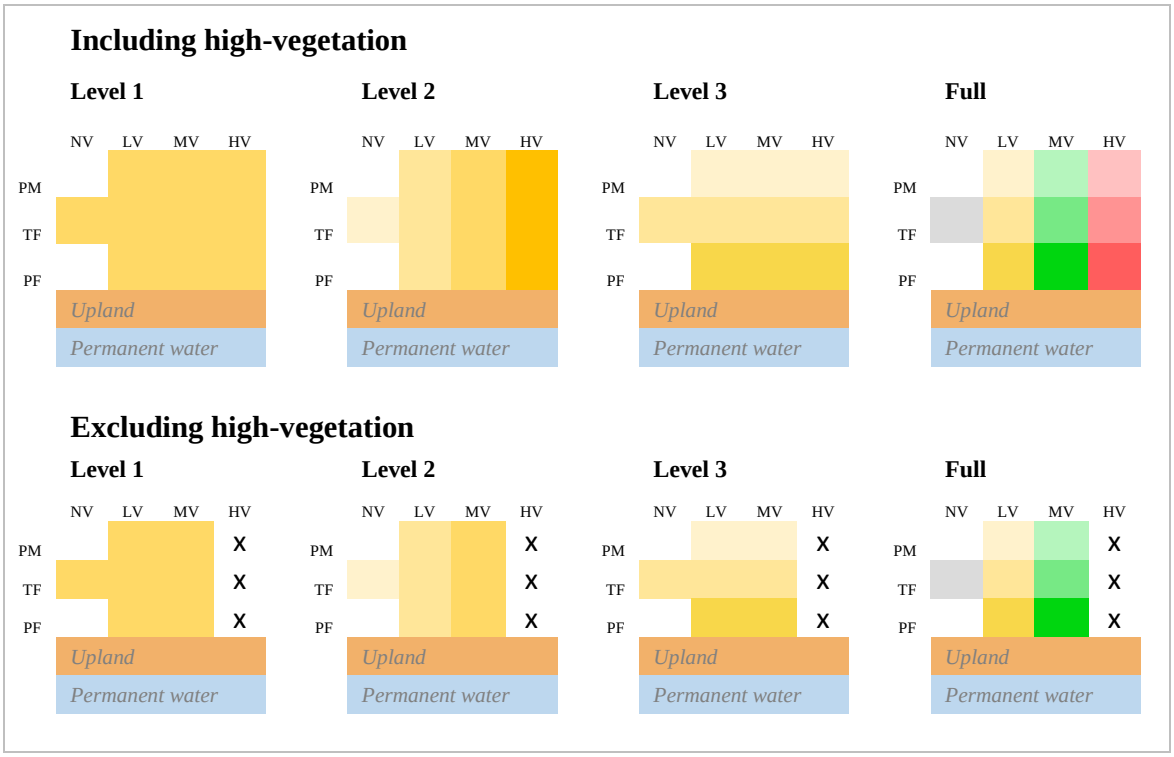

Figure 11: Graphical overview of classes in the different levels. Colour differences indicate the class delineations. NV = non-vegetated, LV = low-vegetated, MV = medium-vegetated, HV = high-vegetated, PM = permanently moist, TF = temporarily flooded, PF = permanently flooded.

3.6 Validation

In order to assess the accuracy of the classifications, the results were validated. All validations were done within R (R Core Team, 2018). The validation measures were the most important outputs, in order to assess the use of Sentinel-1 time series data for wetland characterisation.

As stated in Chapter 3.5.1, for each run in the Monte Carlo simulation of the Random Forest classifications, the random sample points were randomly split in classification- and validation subsets. The 30% used for validation corresponded to 60 validation points per class in each run. After the classification, which was done with the other 70% of the random sample points, the classified wetland types were extracted for the validation locations and compared with the actual wetland types. Per classification, this created 100 accuracy assessments of the 100 Random Forest classifiers, independent from the training data. The following outputs were produced for validation.

Confusion matrix

The confusion matrix is a display of the amount of correctly classified and incorrectly classified objects, within the 30% of the validation points. The rows and columns in a

confusion matrix represent the classes predicted by the classifier and the actual classes. The predicted classes are the classifications made by the Random Forest and the actual classes are the labels which are given to the random sample locations conforming the reference data. For each classification a confusion matrix was produced 100 times, one for each run in the Monte Carlo simulation. The sum of these matrices was taken as a final confusion matrix.

Overall accuracy

The overall accuracy (OA) is derived from the confusion matrix and is an indicator of the number of pixels that is correctly classified by the classifier. It is calculated as a percentage, by dividing the number of correctly classified validation points by the total number of validation points.

Producer's accuracy

The producer's accuracy (PA) is derived from the confusion matrix and is an indicator for the classification accuracy from the point of view of the producer. It is calculated by dividing the number of correctly classified validation points in each class by the number of reference points that are in reality within that class. This percentage represents how well reference pixels of the class are classified.

User's accuracy

The user's accuracy (UA) is derived from the confusion matrix and is an indicator for the classification accuracy from the point of view of the user. It is calculated by dividing the number of correctly classified points in each class by the number of reference points that were classified within that class. This percentage represents the probability of a pixel being classified into a class that actually represents that pixel.

Mode frequency map

In addition to the accuracy measurements based on the validation data, a mode frequency map was generated to indicate the spatial robustness of the classification outputs throughout the entire study area. These maps display for each pixel the number of times this pixel was classified as the resulting mode of the 100 classifications. This indicates the classification consistency per pixel.

Mean mode frequency per class

A mean mode frequency (MMF) per output class was calculated to indicate the robustness per class throughout the 100 classifications. The MMF was calculated by averaging the per-pixel mode frequency for each output class. This measurement indicates an overall robustness per class in the output classifications. An advantage of this measure is that it is not limited to the use of separate validation points and provides a robustness indicator for the entire study area.

4 Results

This chapter describes the results of the 12 distinct Monte Carlo-based Random Forest wetland classifications within the St. Lucia wetlands. The validations of the results are outlined per level in Chapters 4.1, 4.2 and 4.3. A complete overview of the results – including maps – can be found in Appendices 3 to 14.

An overview of the OAs of the classifications can be found in Figure 12. The maps produced with the combination of Sentinel-1 and Sentinel-2 obtained a much higher OA than the maps produced with Sentinel-1 alone. Also, the exclusion of high-vegetated wetlands led to higher accuracies, especially when solely using Sentinel-1.

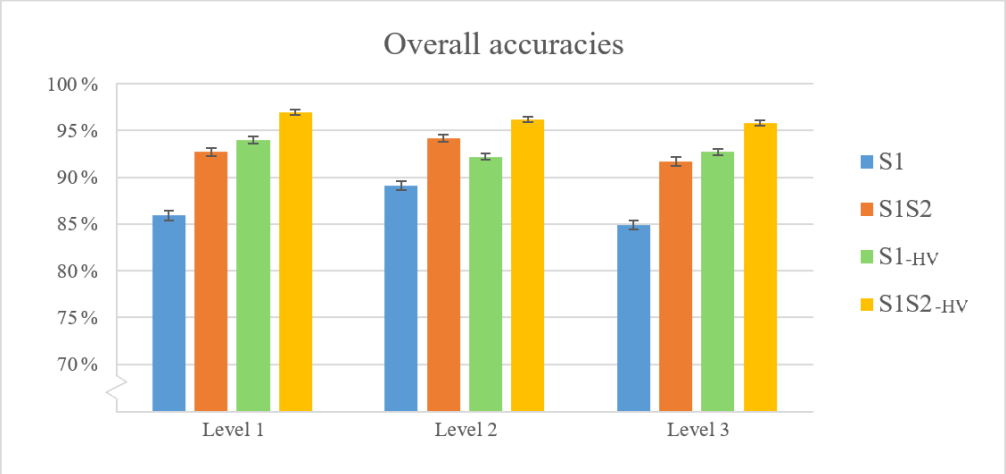

Figure 12: Mean OAs of the Monte Carlo classifications and their 95% confidence intervals based on the 100 runs. Confidence intervals were all <1%.

The level-based outputs of the four classification methods (S1, S1S2, $S1_{-HV}$ and $S1S2_{-HV}$), were overlaid to obtain the final maps for each classification. These final maps can be found in Figure 13.

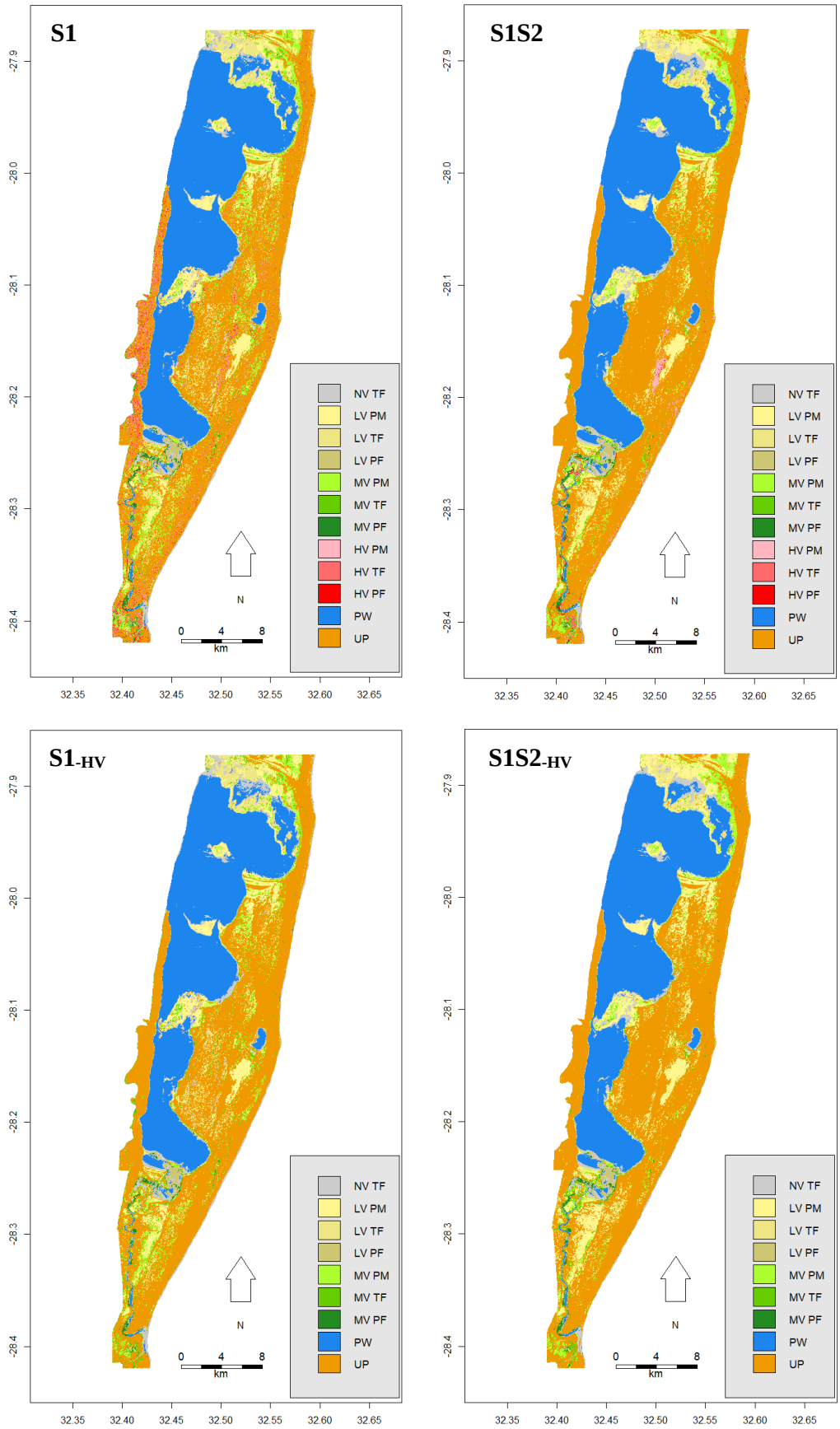

Figure 13: Overlaid maps of all levels in each classification. NV = non-vegetated, LV = low-vegetated, MV = medium-vegetated, HV = high-vegetated, PM = permanently moist, TF = temporarily flooded, PF = permanently flooded, PW = permanent water, UP = upland.

4.1 Level 1 – General Wetland Delineation

An accuracy overview of the Level 1 classifications can be found in Table 13. A full overview of these classifications can be found in Appendices 3, 4, 5 and 6. The OAs of these classifications ranged from 85.9% for S1 to 97.0% for S1S2$_{-HV}$.

Table 13: Accuracy assessments of the Level 1 classifications. OA = Overall Accuracy (%), PA = Producer's Accuracy (%), UA = User's Accuracy (%), MMF = Mean Mode Frequency.

	S1			**S1S2**			**S1$_{-HV}$**			**S1S2$_{-HV}$**		
	OA:	**85.9**		OA:	**92.7**		OA:	**94.0**		OA:	**97.0**	
	PA	UA	MMF	PA	UA	MMF	PA	UA	MMF	PA	UA	MMF
Pmt. water	99.3	97.9	99.6	100	99.6	99.4	99.4	98.2	99.4	100	99.7	99.5
Upland	81.4	78.7	93.8	93.4	86.2	96.0	92.4	91.4	96.9	97.9	93.8	97.0
Wetland	77.1	81.1	92.6	84.7	92.7	93.9	90.3	92.5	95.2	93.2	97.8	95.3

The S1 classification (Appendix 3) obtained an OA of 85.9%. Confusion was observed mainly for the classes upland and wetland. There was a small overestimation of upland and underestimation of wetlands in the classification. Errors were mainly caused by the confusion between high-vegetated wetlands and upland forests. Visual interpretation of the output map and the mode frequency map showed this confusion especially at the western shore of the lake (approximately at -28.25 to -28.00 degrees latitude). This forested upland area was often wrongly classified as a wetland and the mode frequency in this area was also relatively low. The variables VH mean and VH median were found to be the most important for this classification.

The inclusion of Sentinel-2 in the S1S2 classification (Appendix 4) led to an OA of 92.7%. Confusion was again observed mainly between the classes upland and wetland, but this confusion was much lower than in the S1 classification. The overestimation of upland at the cost of wetland was relatively large though. The indices NDVI and MNDWI, derived from the Sentinel-2 data, were found to be more important than the variables from Sentinel-1 for this classification.

The exclusion of high-vegetated areas in the S1$_{-HV}$ classification (Appendix 5) led to an OA of 94.0%. The confusion between upland and wetland was much lower than in the S1 classification. Visual interpretation of the output map and mode frequency map showed the improvements especially at the western shore of the lake, where the upland forests were now more consistently classified correctly as upland. Visual interpretation of the output map also showed that most of the high-vegetated wetlands were now classified as upland. Just as in the

S1 classification, the variables VH mean and VH median were found to be the most important for this classification.

The highest OA was obtained in the S1S2$_{-HV}$ classification (Appendix 6), namely 97.0%. Again, most of the high-vegetated wetlands were now classified as upland. The overestimation of upland at the cost of wetland was still relatively large. The NDVI variables were found to be the most important for this classification.

4.2 Level 2 – Vegetation Types

An accuracy overview of the Level 2 classifications can be found in Table 14. A full overview of these classifications can be found in Appendices 7, 8, 9 and 10. The OAs of these classifications ranged from 89.1% for S1 to 96.2% for S1S2$_{-HV}$.

Table 14: Accuracy assessments of the Level 2 classifications. OA = Overall Accuracy (%), PA = Producer's Accuracy (%), UA = User's Accuracy (%), MMF = Mean Mode Frequency.

	S1			**S1S2**			**S1$_{-HV}$**			**S1S2$_{-HV}$**		
	OA:	**89.1**		OA:	**94.2**		OA:	**92.2**		OA:	**96.2**	
	PA	UA	MMF	PA	UA	MMF	PA	UA	MMF	PA	UA	MMF
Non-veg.	99.2	98.4	98.0	99.6	98.5	98.8	99.3	98.6	98.2	99.5	98.3	98.5
Low-veg.	92.3	86.9	95.6	96.3	94.0	96.2	91.4	86.6	95.5	96.2	93.7	96.5
Med.-veg.	75.9	91.0	92.8	88.7	88.8	94.2	85.8	91.7	94.9	92.9	96.7	94.7
High-veg.	88.9	89.5	95.7	92.1	95.3	96.5	*NA*	*NA*	*NA*	*NA*	*NA*	*NA*

The S1 classification (Appendix 7) obtained an OA of 89.1%. Confusion was observed mainly for the class medium-vegetated wetland, which was confused with the classes low- and high-vegetated wetland and was severely underestimated.

The inclusion of Sentinel-2 in the S1S2 classification (Appendix 8) led to an OA of 94.2%. Compared with the S1 classification, the confusion for the class medium-vegetated wetland was much lower.

The exclusion of high-vegetated areas in the S1$_{-HV}$ classification (Appendix 9) led to an OA of 92.2%. Still, confusion occurred for the classes low-vegetated wetland and medium-vegetated wetland. The amount of low-vegetated wetland was overestimated at the cost of medium-vegetated wetland.

Also in this level the highest OA was obtained in the S1S2$_{-HV}$ classification (Appendix 10), namely 96.2%. The variables VH mean and VV minimum were found to be the most important for all classifications in Level 2.

4.3 Level 3 – Surface Water Dynamics

An accuracy overview of the Level 2 classifications can be found Table 15. A full overview of these classifications can be found in Appendices 11, 12, 13 and 14. The OAs of these classifications ranged from 84.9% for S1 to 95.8% for S1S2$_{-HV}$.

Table 15: Accuracy assessments of the Level 3 classifications. OA = Overall Accuracy (%), PA = Producer's Accuracy (%), UA = User's Accuracy (%), MMF = Mean Mode Frequency.

	S1			**S1S2**			**S1$_{-HV}$**			**S1S2$_{-HV}$**		
	OA:	**84.9**		OA:	**91.7**		OA:	**92.7**		OA:	**95.8**	
	PA	UA	MMF	PA	UA	MMF	PA	UA	MMF	PA	UA	MMF
Pmt. moist	86.8	86.5	95.3	96.0	93.0	97.5	92.1	91.1	96.6	96.5	94.7	97.9
Temp. fl.	82.5	77.8	92.4	89.2	87.9	95.2	89.3	88.9	95.7	92.6	94.8	96.1
Pmt. fl.	85.3	91.1	88.4	89.9	94.2	93.9	96.7	97.3	97.5	98.1	97.8	97.0

The S1 classification (Appendix 11) obtained an OA of 84.9%. Confusion was observed mainly for the class temporarily flooded wetland, which was overestimated at the cost of permanently flooded wetland. The class permanently flooded wetland also had a relatively low MMF throughout the 100 classifications, indicating a poor robustness of classification.

The inclusion of Sentinel-2 in the S1S2 classification (Appendix 12) led to an OA of 91.7%. Especially the MMF of the class permanently flooded wetland improved, indicating a more consistent classification for this class. This class was again underestimated though, due to being wrongly classified as temporarily flooded wetland.

The exclusion of high-vegetated areas in the S1$_{-HV}$ classification (Appendix 13) led to an OA of 92.7%. Especially the confusion between the classes temporarily flooded wetland and permanently flooded wetland was reduced here. Also, the MMF of the class permanently flooded wetland was much higher, indicating a more robust classification. Confusion was observed mainly for the class temporarily flooded wetland.

The highest OA was obtained in the S1S2$_{-HV}$ classification (Appendix 14), namely 95.8%. Although in relatively small amounts, confusion has been observed here mainly for the classes permanently moist wetland and temporarily flooded wetland. The mean and median values for NDPI and VVrVH were found to be the most important for all classifications in Level 3.

5 Discussion

The results presented in Chapter 4 give a comprehensive insight in the capabilities of Sentinel-1 time series data and the combined use of Sentinel-1 and Sentinel-2 for wetland characterisation. In this chapter the main findings and limitations of this research are discussed. Also, the results are discussed in the perspective of findings in previous studies. In Chapter 5.1 the results are discussed per level of classification. In Chapter 5.2 the main findings are summarised. Chapter 5.3 outlines the main limitations for the used methodology.

5.1 Level-Based Findings

5.1.1 Level 1 – General Wetland Delineation

In all Level 1 classifications, confusion was mainly observed for the classes wetland and upland, where upland was often overestimated at the cost of wetland. The results of the S1 classification showed an OA of 85.1%. However, visual interpretation of the output map revealed that the confusion of the classes wetland and upland was likely to be much higher than the accuracy measurements indicated. The confusion was especially observed between upland forests and high-vegetated wetlands. Besides the confusion, visual interpretation of the mode frequency map pointed out the inconsistency for classifying high-vegetated areas either as upland or wetland when using Sentinel-1. This indicates that C-band operating in VV/VH mode has a low capacity to capture backscattering differences between upland forests and high-vegetated wetlands, such as swamp- or mangrove forests. The occurrence of these high-vegetated wetlands in an area obviously causes a disturbance for general wetland delineation when using Sentinel-1. This finding is in line with Mahdianpari et al. (2018), who observed the highest confusion between swamp forests (with a PA of 57% in a pixel-based classification) and upland when using Sentinel-1. Their OA obtained for general wetland delineation using Sentinel-1 was 85% (this percentage was derived from their presented confusion matrices by calculating only the confusion between four wetland and four upland classes), and thus very similar to the OA obtained in this research.

The assumption of Sentinel-1 being incapable of delineating high-vegetated wetlands is underlined by the validation of the $S1_{-HV}$ classification. The large accuracy improvement here (85.9% to 94.0%) was caused by the decreased confusion between high-vegetated wetlands and upland forests. Also, the mode frequency map revealed a better robustness for high-vegetated areas. This proves again that high-vegetated wetlands contributed largely to confusion in the S1 classification. Most of the high-vegetated wetlands, which were not included in this classification, were now classified as uplands because they were considered as upland forests. The $S1_{-HV}$ classification shows the good capabilities of Sentinel-1 for general wetland delineation, provided that only herbaceous and shrubby wetlands occur in an area. However, this finding is contradicted by Mleczko & Mróz (2018), who used Sentinel-1 time

series data for classifications in herbaceous wetlands and concluded that Sentinel-1 obtains relatively poor accuracies (with an OA of 65% for mapping six classes) for this purpose. They obtained better accuracies with the use of dual- and quad-polarimetric X-band radar in herbaceous wetlands, because this short wavelength was better at observing double-bounce scattering from grasses and reeds.

The accuracy improvement (85.9% to 92.7%) with the inclusion of Sentinel-2 data in the S1S2 classification was relatively high. Especially the confusion between the classes upland and wetland decreased. The MDG scores for the optical variables NDVI and MNDWI were also higher than for the radar variables. This proves that the inclusion of optical data besides Sentinel-1 data leads to a significant accuracy improvement for general wetland delineation and that the variables obtained from optical data have a high stake in this. The importance of the NDVI for general wetland delineation can be explained by the fact that this index includes the NIR reflectance, which is considered to be an important measure for wetland delineation (Mahdavi et al., 2018).

As expected, when applying both these accuracy improving features – the exclusion of high-vegetated areas and the inclusion of optical data – in the $S1S2_{-HV}$ classification, the highest accuracy (97.0%) was obtained.

Several past studies have attempted general wetland delineation, sharing methodological similarities with this research, but using different satellite systems than Sentinel-1. Past studies obtained OAs ranging from 85% to 92% for general wetland delineation using both optical and radar data (Corcoran et al., 2013; Mahdianpari et al., 2017; Töyrä et al., 2002; Wright & Gallant, 2007). Compared to these studies, the OAs obtained in this research were relatively good.

5.1.2 Level 2 – Vegetation Types

In all Level 2 classifications, confusion was mainly observed for the class medium-vegetated wetland. This class was relatively often confused with low- and high-vegetated wetland. This confusion was the highest in the S1 classification. The high confusion for the class medium-vegetated wetland – where shrubby vegetation is dominant – can be explained by the ordinal nature of the used classes, where this class falls in between the classes low- and high-vegetated wetland. The high confusion for shrubby-vegetated areas with other vegetation types is a known phenomenon for land cover classifications in general (Tsendbazar et al., 2016).

The accuracy improvement (89.1% to 94.2%) with the inclusion of Sentinel-2 in the S1S2 classification was relatively high. Despite this accuracy improvement, the importance of the Sentinel-2 variables was not observed in the MDG scores. It was expected that the NDVI

would have a higher importance for characterising wetland vegetation types. However, the Sentinel-1 variables were still the most important for this classification.

The exclusion of high-vegetated wetlands in the $S1_{-HV}$ classification led to a small accuracy improvement (89.1% to 92.2%). This improvement was mainly caused by the exclusion of a class, which reduced the number of considered classes from three to four. Obviously, this contributed to an accuracy improvement, because the confusion between the classes medium- and high-vegetated wetland was completely removed.

The highest accuracy (96.2%) was obtained when Sentinel-2 was included and high-vegetated areas were excluded in the $S1S2_{-HV}$ classification. The accuracy improvement relative to the S1S2 classification was again mainly caused by the exclusion of a class. Also here, a high importance of optical variables was not observed. The high MDG scores for the Sentinel-1 variables in all Level 2 classifications indicate the importance of Sentinel-1 for mapping wetland vegetation types. Although the inclusion of Sentinel-2 improves the accuracy, Sentinel-1 has the highest stake in accurately mapping wetland vegetation types.

The accuracy obtained with Sentinel-1 only (89.1%) and the MDG scores of its variables were relatively high in Level 2, when compared with classification levels 1 and 3. This implies that the classification of wetland vegetation types can be done relatively accurate with Sentinel-1. As the importance of the variables VH mean and VV minimum was high, it is likely that volume scattering (especially for VH in medium- and high-vegetated wetland), double-bounce scattering (especially for VV in low- and medium-vegetated wetland) and specular reflection (especially for VV in low- and non-vegetated wetland) is well observed with Sentinel-1 and contributes to accurate classifications of wetland vegetation types. It should be noted that the masking out of permanent water and especially upland prior to this classification also contributed to a better accuracy in this level, because the classification was demarcated to mapping only wetland vegetation types and confusion with upland vegetation types could not occur.

5.1.3 Level 3 – Surface Water Dynamics

The results of the S1 classification for surface water dynamics showed an OA of 84.9%, with the most inaccurate classification for temporarily flooded wetland. The class permanently flooded wetland had a low MMF, which indicates that this class was classified relatively inconsistent throughout the 100 classifications.

An important note for the S1 classifications in Level 3 is that the confusion between high-vegetated wetlands and upland forests in Level 1 forced the classification of surface water dynamics for areas that were misclassified as wetlands in this preceding level. This may have caused confusion for the S1 classification in Level 3, which could be traced back to errors

already made in Level 1. This is especially visible at the western shore of the lake, where low mode frequencies were obtained also in Level 3, because the classifier was forced to make meaningless classifications for surface water dynamics in upland areas.

Also in this classification level, the accuracy improvement (84.9% to 91.7%) with the inclusion of Sentinel-2 data in the S1S2 classification was relatively high. Also, the MMF improvement of the class permanently flooded wetland implies more robustness for this class when Sentinel-2 data is used besides Sentinel-1 data.

An even larger accuracy improvement (84.9% to 92.7%) was observed with the exclusion of high-vegetated areas in the $S1_{-HV}$ classification. The MMF increase for the class permanently flooded wetland (88.4 to 97.5) was striking. On the one hand, these accuracy improvements were caused by a more accurate wetland delineation in the preceding $S1_{-HV}$ classification in Level 1. On the other hand, the improvements prove again the incapability of Sentinel-1 to map high-vegetated wetlands. In this case, the performance is poor for distinguishing classes of surface water dynamics in high-vegetated wetlands.

As expected, the highest accuracy was also here observed for the $S1S2_{-HV}$ classification. For all classifications in level 3, the highest MDG scores were obtained by the VVrVH and NDPI variables. The high importance of the VVrVH and NDPI can be explained by the fact that the plain C-band measurements of VV and VH are mostly dominated by backscatter mechanisms of vegetation, and not by moisture or occurrence of water. When attempting a classification of surface water dynamics, this results in a high within-class variance for VV and VH variables. Apparently, the ratio and normalised difference between VV and VH are better at capturing differences in surface water dynamics. An unexpected result in all classifications in Level 3 was that the standard deviations for both the Sentinel-1 and Sentinel-2 variables were relatively unimportant for classifying surface water dynamics.

In past studies using different satellite systems than Sentinel-1, the classification of wetland vegetation types and surface water dynamics have often been integrated. Past studies that share methodological similarities with the Level 2 and Level 3 classifications in this research obtained OAs ranging from 81% to 90% for this purpose (Hess et al., 2003; Martinez & Le Toan, 2007; Töyrä & Pietroniro, 2005). Compared to these studies, the OAs obtained in this research were relatively good.

5.2 Main Findings

The results obtained in all levels with the sole use of Sentinel-1 showed accuracies in the range of 84.9% to 89.1%. However, high confusions were observed for classifications within high-vegetated areas. In the Level 1 classifications, the use of Sentinel-1 data did not suffice to distinguish upland forests and high-vegetated wetlands. This indicates that the C-band

Sentinel-1 sensors cannot capture backscattering differences between these land cover types. In the Level 3 classifications, Sentinel-1 also seemed to be insufficient for classifying surface water dynamics in high-vegetated wetlands. The incapability of Sentinel-1 for mapping high-vegetated wetlands is not surprising. Although C-band radar depending on VV mode has shown a moderate capability of mapping high-vegetated wetlands in the past (Kasischke & Bourgeau-Chavez, 1997; Townsend, 2002; Wang et al., 1995), both this wavelength and polarisation are inferior to the use of longer wavelengths such as L-band, and HH mode for this purpose (Baghdadi et al., 2001; Brisco et al., 2011; Henderson & Lewis, 2008; Townsend, 2002; Wang et al., 1995).

The inclusion of optical data from Sentinel-2 largely improved the accuracies in all levels of wetland classification. The NDVI and MNDWI had a high stake in this improvement especially for general wetland delineation. Despite optical data being determined to be insufficient for wetland mapping (Bourgeau-Chavez et al., 2009; Ozesmi & Bauer, 2002), this proves that optical data does have a significant added value in a combined use with Sentinel-1 in wetland classifications. This is substantiated by Mahdianpari et al. (2018), who studied the combined use of Sentinel-1 and Sentinel-2 for wetland mapping and proved the added value of Sentinel-2. It is notable that they even observed higher OAs for wetland mapping with the sole use of Sentinel-2 than with the sole use of Sentinel-1. However, they did not classify dynamic aspects in wetlands, such as surface water dynamics or flood frequencies, demanding a high-temporal density Sentinel-2 cannot deliver.

Although its added value was showed in this research, the use of optical data has limitations when being used for more detailed multi-temporal analyses. For the classification of wetlands into only three classes of surface water dynamics, the temporal density of the quarterly composites of Sentinel-2 images was sufficient. However, for more detailed temporal classifications, such as classifications of flood frequencies as done by Huang et al. (2017), Tian et al. (2017) and Xing et al. (2018), the use of optical data will be limited, especially in areas that are subject to periods of persistent cloud-cover.

Despite the fact that the inclusion of optical data led to accuracy improvements in all classification levels, the Sentinel-1 variables remained the most important in Level 2 and Level 3. This implies a high stake of Sentinel-1 time series data in accurately mapping wetland vegetation types and surface water dynamics. Sentinel-1 only was especially accurate (with an OA of 89.1%) for mapping wetland vegetation types.

5.3 Limitations

A main limitation in the used methods is that the calculated accuracies of the classification outputs may have been overestimated due to spatial autocorrelation among training- and validation data. This may have happened because reference points were randomly split into

training- and validation subsets. As the reference points were selected with reference sample polygons as stratification, the likeliness of spatial autocorrelation between training- and validation data was the highest for classes which were spatially underrepresented in the study area. Examples of such classes are non-vegetated wetland and permanently flooded wetland. For these classes, which cover only small parts of the study area, training- and validation points were more clustered than for larger classes, such as upland or permanent water. In these larger classes, the reference points were more sparsely distributed. As a result, spatial autocorrelation has probably not been problematic for the Level 1 classifications, but might have been for the more detailed Level 2 and Level 3 classifications. To ensure a better statistical accuracy of the maps, more independency between training- and validation data is needed, meeting the requirements of stage 3 in the CEOS Validation Hierarchy (CEOS-WGCV Land Product Validation Subgroup, 2019). Also, a proper validation of the final overlaid maps (Figure 13) could not be done, because no additional independent validation data was collected for this purpose.

Additional accuracy overestimations may have occurred due to the use of specific reference sample polygons as stratification for the sample points. As a result, the reference frame and the study area did not match. Most of the chosen reference sample polygons were areas that could obviously be appointed to a certain class, while areas that were more difficult to appoint to a class have often been neglected. In Random Forest classifications, this results in purer splits of the variables and thus higher classification accuracies, while the ground-truth can be more complex. Acquiring sample points throughout the entire study area would result in more representative reference data, and thus a more reliable validation (Congalton, 1988).

Another limitation for the used research methodology is the reference data collection process. High-resolution aerial- and satellite images have been the main source of information for collecting reference samples. Because no detailed study of the ground-truth in the study area was done, errors may have occurred during this process. Still, the use of high-resolution aerial and satellite images for reference data collection is a widely adopted and accepted method for land cover classifications (Lesiv et al., 2018). The alternative of an on-site research for reference data collection would be extremely time-consuming for a large study area, especially when multi-temporal data needs to be collected.

The limitations for the collection of detailed reference data also resulted in a limitation for the number of distinguishable classes in the used classification scheme. Especially in the Level 3 classification, where only three classes of surface water dynamics were distinguished, a more detailed classification might have revealed the capabilities of the temporally dense Sentinel-1 data in a better way. For example, a classification of flood frequencies would be more challenging for the time series data and might have emphasised more superiority of the temporally dense Sentinel-1 data over the limited Sentinel-2 data. The incorporation of

classification methods used by Huang et al. (2017), Tian et al. (2017) and Xing et al. (2018) for characterising surface water dynamics can be useful for a more detailed assessment of Sentinel-1 data. Their methods were mainly based on the classification of single images within a time series and detecting changes, instead of a classification based on temporal statistics obtained from an entire time series.

As only the indices NDVI and MNDWI have been used as optical variables, the added value of optical data besides Sentinel-1 may have been underestimated. According to Mahdavi et al. (2018), the red-edge and NIR are valuable single-band measures for wetland delineation when using optical data. In this research, the NIR reflectance was only used as a reflectance measure within the NDVI. The red-edge reflectance, which is also measured by Sentinel-2, was not used.

The used spatial resolution for the classifications in this research was 30 metres. Despite this resolution being relatively high for wetland mapping, a drawback is that the full resolution of Sentinel-1 (10 metres) was not used. This was done to reduce the processing time for the classifications.

Several issues come forward regarding the scalability of the used methods for practical applications in wetland monitoring. While the platform GEE has proven to be a valuable tool for pre-processing and integrating great numbers of both radar and optical satellite images, the use of R was preferred over GEE for classifications. This limits the scalability of the used methods. Although R has more advanced options for classifications than GEE, a method using solely GEE would be easier applicable for large-scale wetland monitoring in practice.

6 Conclusion

The newly available Sentinel-1 radar data, which is available free of charge, has a relatively high spatial and temporal resolution and therefore provides a unique opportunity for more accurate wetland monitoring from space. This research aimed at assessing the use of dense Sentinel-1 radar time series data for mapping and characterising different wetland types. This was done by assessing the sole use of Sentinel-1 time series data and the combined use of Sentinel-1 with complementary optical data, namely Sentinel-2 data. Sentinel-1 was critically assessed for its capabilities in mapping complex wetland characteristics, occurring in higher-vegetated wetlands and wetlands with dynamicity in surface water. The research questions and brief answers to them are outlined below.

1. *How accurate can wetlands be mapped within different levels of characterisation, using Sentinel-1 time series data?*

The accuracy of wetland mapping with Sentinel-1 time series data varies per characterisation level. Sentinel-1 is found to be suitable for accurate classification of wetland vegetation types. For general wetland delineation and classifying surface water dynamics, inaccuracies are observed mainly for high-vegetated areas. Better accuracies are obtained when characterising areas with only herbaceous- or shrubby vegetated wetlands.

2. *What is the accuracy improvement for wetland characterisation when combining Sentinel-1 time series data with optical data from Sentinel-2?*

The incorporation of optical data from Sentinel-2 besides Sentinel-1 leads to significant accuracy improvements, observed at all levels of wetland characterisation. Sentinel-2 was particularly valuable for general wetland delineation. However, the usefulness of optical data is limited for mapping characteristics that demand a higher temporal density, such as flood frequencies.

3. *How and to what extent are the accuracies of the produced maps affected by the complexities in wetland characteristics?*

Mapping high-vegetated wetlands using Sentinel-1 data was found to be inaccurate as a high confusion was observed between upland forests and high-vegetated wetlands. Also, the complexity in wetland's surface water dynamics affect the accuracies of maps produced with Sentinel-1, both for temporarily flooded and permanently flooded wetlands. Among these, high-vegetated wetlands subject to permanent or temporary flooding cause a considerable confusion in the classifications. The combined use of Sentinel-1 and Sentinel-2 helps to address the complexity in wetland characteristics and obtains better accuracies.

A main finding in this research is that Sentinel-1 time series data gives sufficient results for mapping low- to medium vegetated wetlands, with mainly herbaceous or shrubby vegetation.

For general wetland delineation and characterising surface water dynamics, accurate maps can be produced within such wetlands. Also, characterising different vegetation types can be done relatively accurate with Sentinel-1. Therefore, it is likely that scatter mechanisms caused by flooding in different types of vegetation are well observed with Sentinel-1.

The use of Sentinel-1 did not suffice to make accurate wetland classifications in high-vegetated areas. The C-band radar systems aboard the Sentinel-1 satellites operating in VV/VH mode have been found to be incapable of distinguishing high-vegetated wetlands from upland forests, because the radar systems have limited capabilities for vegetation penetration and observing double-bounce scattering. Mapping surface water dynamics with Sentinel-1 is also relatively inaccurate in high-vegetated wetlands. These inaccuracies are largely reduced when high-vegetated wetlands are left out in classifications. Another finding in this research is that the inclusion of optical data from Sentinel-2 improves the map accuracies significantly at all levels of wetland characterisation. Especially for general wetland delineation, optical data has a high stake in this.

As discussed in this research, a main shortcoming of Sentinel-1 radar for wetland characterisation is its C-band system. The use of an L-band system has shown better mapping results in the past, especially due to its capabilities for mapping high-vegetated wetlands. Regarding the usefulness of different wavelengths, the use of the large-wavelength P-band system aboard the BIOMASS satellite will also be promising for wetland monitoring in the future. Another limitation of the Sentinel-1 sensors is that they do not acquire data in quad-polarimetric mode. They do also not use the HH/HV mode over non-polar land, which is determined to have better capacities for wetland mapping.

This study provided a comprehensive assessment of Sentinel-1 radar time series data for wetland mapping and characterisation, in a way that had not been researched before. The relatively high spatial and temporal resolutions of this new C-band dual-polarimetric radar system were tested in a study area. Besides presenting several main findings regarding the use of Sentinel-1 data, this research also produced several accurate wetland maps for the St. Lucia wetlands. Also, four generically applicable methods for wetland characterisation by using Sentinel-1 and Sentinel-2 data were presented.

A main limitation in this research was the possible dependency among training- and validation data. This may have caused accuracy overestimations for the validation of the produced maps. In order to obtain more reliable validations, more independency of training samples should be ensured. Also, the use of reference data that represents the entire study area is better to obtain more reliability in validations. Another limitation in this research was the lack of detailed ground-truth data. This resulted in the use of a rather simplistic classification scheme and may have resulted in errors in the reference data collection process. For future research, the use of

high-resolution images acquired at multiple dates (e.g. using unmanned aerial vehicles) should provide more detailed reference data. The use of on-site measurements for multiple dates will most likely be too time-consuming, although very valuable. With the availability of more detailed ground-truth data, it is advised to make use of an extended classification for surface water dynamics in wetlands, in order to truly test the capacities of Sentinel-1 time series data. An extended classification for surface water dynamics can also be done with the absence of more detailed reference data, when time series analyses are done with per-image classifications. Another recommendation for future research is to exploit the added value of optical data in a better way, by incorporating individual band measures for the red-edge or NIR reflectance.

In conclusion, the high spatial and temporal resolution images and free data access of Sentinel-1 provide a great opportunity towards operational wetland monitoring. Despite its shortcomings for mapping high-vegetated wetlands and extra advantages contributed by Sentinel-2 data, Sentinel-1 data has proven to be a valuable mean for wetland characterisation.

7 References

Ainsworth, T. L., Kelly, J. P., & Lee, J. S. (2009). Classification comparisons between dual-pol, compact polarimetric and quad-pol SAR imagery. *ISPRS Journal of Photogrammetry and Remote Sensing*. https://doi.org/10.1016/j.isprsjprs.2008.12.008

Amler, E., Schmidt, M., & Menz, G. (2015). Definitions and mapping of East African Wetlands: A Review. *Remote Sensing*, *7*(5), 5256–5282. https://doi.org/10.3390/rs70505256

Baghdadi, N., Bernier, M., Gauthier, R., & Neeson, I. (2001). Evaluation of C-band SAR data for wetlands mapping. *International Journal of Remote Sensing*, *22*(1), 71–88. https://doi.org/10.1080/014311601750038857

Bourgeau-Chavez, L. K., Riordan, K., Powel, R., Miller, N., & Nowels, M. (2009). Improving Wetland Characterization with Multi-Sensor, Multi-Temporal SAR and Optical/Infrared Data Fusion. In *Advances in Geoscience and Remote Sensing*. https://doi.org/10.5772/8327

Bourgeau-Chavez, L. L., Smith, K. B., Brunzell, S. M., Kasischke, E. S., Romanowicz, E. a., & Richardson, C. J. (2005). Remote monitoring of regional inundation patterns and hydroperiod in the Greater Everglades using Synthetic Aperture Radar. *Wetlands*, *25*(1), 176–191.

Breiman, L. (2001). Random Forests. *Machine Learning*, *45*, 5–32.

Brisco, B., Kapfer, M., Hirose, T., Tedford, B., & Liu, J. (2011). Evaluation of C-band polarization diversity and polarimetry for wetland mapping. *Canadian Journal of Remote Sensing*. https://doi.org/10.5589/m11-017

Bunn, S. E., Boon, P. I., Brock, M. A., & Schofield, N. J. (1997). *National Wetlands R&D Program: Scoping Review*. Canberra.

Cazals, C., Rapinel, S., Frison, P.-L., Bonis, A., Mercier, G., Mallet, C., … Rudant, J.-P. (2016). Mapping and Characterization of Hydrological Dynamics in a Coastal Marsh Using High Temporal Resolution Sentinel-1A Images. *Remote Sensing*, *8*(7), 570. https://doi.org/10.3390/rs8070570

CEOS-WGCV Land Product Validation Subgroup. (2019). CEOS Validation Hierarchy. Retrieved February 17, 2019, from https://lpvs.gsfc.nasa.gov/index.html

Chatziantoniou, A., Petropoulos, G. P., & Psomiadis, E. (2017). Co-Orbital Sentinel 1 and 2 for LULC mapping with emphasis on wetlands in a mediterranean setting based on machine learning. *Remote Sensing*, *9*(12). https://doi.org/10.3390/rs9121259

Chen, P. Y., Srinivasan, R., Fedosejevs, G., Báez-González, A. D., & Gong, P. (2002). Assessment of NDVI Composites Using Merged NOAA-14 and NOAA-15 AVHRR Data. *Geographic Information Sciences*. https://doi.org/10.1080/10824000209480571

Clint Slatton, K., Crawford, M. M., & Chang, L. Der. (2008). Modeling temporal variations

in multipolarized radar scattering from intertidal coastal wetlands. *ISPRS Journal of Photogrammetry and Remote Sensing*. https://doi.org/10.1016/j.isprsjprs.2008.07.003

Clulow, A. D., Everson, C. S., Price, J. S., Jewitt, G. P. W., & Scott-Shaw, B. C. (2013). Water-use dynamics of a peat swamp forest and a dune forest in Maputaland, South Africa. *Hydrology and Earth System Sciences*. https://doi.org/10.5194/hess-17-2053-2013

Congalton, R. (1988). A comparison of sampling schemes used in generating error matrices for assessing the accuracy of maps generated from remotely sensed data. *Photogrammetric Engineering and Remote Sensing*.

Corcoran, J. M., Knight, J. F., & Gallant, A. L. (2013). Influence of multi-source and multi-temporal remotely sensed and ancillary data on the accuracy of random forest classification of wetlands in northern Minnesota. *Remote Sensing*, *5*(7), 3212–3238. https://doi.org/10.3390/rs5073212

Council for Scientific and Industrial Research. (2011a). NFEPA wetlands.

Council for Scientific and Industrial Research. (2011b). NFEPA wetlands vegetation.

Cowardin, L. M., Carter, V., Golet, F. C., & La Roe, E. T. (1979). Classification of Wetlands and Deepwater Habitats of the United States. *Northern Prairie Wildlife Research Center Online.*

European Space Agency. (2015). Coulour vision for Copernicus. The story of Sentinel-2. Retrieved from http://esamultimedia.esa.int/multimedia/publications/ESA-Bulletin-161/offline/download.pdf

European Space Agency. (2017a). Sentinel-1 data. *Derived from and Processed by: Google Earth Engine*.

European Space Agency. (2017b). Sentinel-2 data. *Derived from and Processed by: Google Earth Engine*.

European Space Agency. (2018). Copernicus, Overview. Retrieved September 15, 2018, from https://www.esa.int/Our_Activities/Observing_the_Earth/Copernicus/Overview3

European Space Agency. (2019). Biomass - ESA Future Missions. Retrieved January 29, 2019, from https://earth.esa.int/web/guest/missions/esa-future-missions/biomass

Farr, T. G., Rosen, P. A., Caro, E., Crippen, R., Duren, R., Hensley, S., … Alsdorf, D. E. (2007). The shuttle radar topography mission. *Reviews of Geophysics*. https://doi.org/10.1029/2005RG000183

Federal Geographic Data Committee. (1997). National Vegetation Classification Standard.

Furtado, L. F. de A., Silva, T. S. F., & Novo, E. M. L. de M. (2016). Dual-season and full-polarimetric C band SAR assessment for vegetation mapping in the Amazon várzea wetlands. *Remote Sensing of Environment*. https://doi.org/10.1016/j.rse.2015.12.013

Gallant, A. L. (2015). The challenges of remote monitoring of wetlands. *Remote Sensing*,

7(8), 10938–10950. https://doi.org/10.3390/rs70810938

Gao, B. C. (1996). NDWI - A normalized difference water index for remote sensing of vegetation liquid water from space. *Remote Sensing of Environment*. https://doi.org/10.1016/S0034-4257(96)00067-3

GeoTerraImage. (2015). South African national land-cover dataset 2013–2014.

Google. (2018a). Google Earth. Google.

Google. (2018b). Google Earth Engine. Retrieved October 6, 2018, from https://earthengine.google.com/

Google. (2018c). Sentinel-1 Algorithms. Retrieved November 11, 2018, from https://developers.google.com/earth-engine/sentinel1

Gumbricht, T., Roman-Cuesta, R. M., Verchot, L., Herold, M., Wittmann, F., Householder, E., … Murdiyarso, D. (2017). An expert system model for mapping tropical wetlands and peatlands reveals South America as the largest contributor. *Global Change Biology*, *23*(9), 3581–3599. https://doi.org/10.1111/gcb.13689

Guo, M., Li, J., Sheng, C., Xu, J., & Wu, L. (2017). A review of wetland remote sensing. *Sensors (Switzerland)*, *17*(4), 1–36. https://doi.org/10.3390/s17040777

Henderson, F. M., & Lewis, A. J. (2008). Radar detection of wetland ecosystems: A review. *International Journal of Remote Sensing*, *29*(20), 5809–5835. https://doi.org/10.1080/01431160801958405

Hess, L. L., & Melack, J. M. (1994). Mapping wetland hydrology and vegetation with synthetic aperture radar. *International Journal of Ecology & Environmental Sciences*.

Hess, L. L., Melack, J. M., Filoso, S., & Wang, Y. (1995). Delineation of Inundated Area and Vegetation Along the Amazon Floodplain with the SIR-C Synthetic Aperture Radar. *IEEE Transactions on Geoscience and Remote Sensing*. https://doi.org/10.1109/36.406675

Hess, L. L., Melack, J. M., Novo, E. M. L. M., Barbosa, C. C. F., & Gastil, M. (2003). Dual-season mapping of wetland inundation and vegetation for the central Amazon basin. *Remote Sensing of Environment*, *87*(4), 404–428. https://doi.org/10.1016/j.rse.2003.04.001

Hess, L. L., Melack, J. M., & Simonett, D. S. (1990). Radar detection of flooding beneath the forest canopy: A review. *International Journal of Remote Sensing*. https://doi.org/10.1080/01431169008955095

Huang, W., Devries, B., Huang, C., Jones, J., Lang, M., & Creed, I. (2017). Automated extraction of inland surface water extent from Sentinel-1 data. *International Geoscience and Remote Sensing Symposium (IGARSS)*, *2017–July*, 2259–2262. https://doi.org/10.1109/IGARSS.2017.8127439

Huete, A., Didan, K., Miura, T., Rodriguez, E. P., Gao, X., & Ferreira, L. G. (2002). Overview of the radiometric and biophysical performance of the MODIS vegetation indices. *Remote Sensing of Environment*. https://doi.org/10.1016/S0034-4257(02)00096-2

iSimangaliso Wetland Park. (2017). iSimangaliso: The restoration of Africa's largest estuarine lake receives a boost. Retrieved November 13, 2018, from https://isimangaliso.com/newsflash/south-africas-largest-wetland-rehabilitation-project-achieves-important-milestone/

Kaplan, G., & Avdan, U. (2018a). Monthly Analysis of Wetlands Dynamics Using Remote Sensing Data. *ISPRS International Journal of Geo-Information*, *7*(10), 411. https://doi.org/10.3390/ijgi7100411

Kaplan, G., & Avdan, U. (2018b). Sentinel-1 and Sentinel-2 Data Fusion for Mapping and Monitoring Wetlands, (July), 1–12. https://doi.org/10.20944/preprints201807.0244.v1

Kasischke, E. S., & Bourgeau-Chavez, L. L. (1997). Monitoring South Florida wetlands using ERS-1 SAR imagery. *Photogrammetric Engineering & Remote Sensing*.

Keddy, P. A. (2010). *Wetland ecology: Principles and conservation*. Cambridge University Press. https://doi.org/10.1017/CBO9780511778179

Keshtkar, H., Voigt, W., & Alizadeh, E. (2017). Land-cover classification and analysis of change using machine-learning classifiers and multi-temporal remote sensing imagery. *Arabian Journal of Geosciences*. https://doi.org/10.1007/s12517-017-2899-y

Kriegler, F. J., Malila, W. A., Nalepka, R. F., & Richardson, W. (1969). Preprocessing transformations and their effects on multispectral recognition. In *Proceedings of the 6th international symposium on remote sensing of environment*. https://doi.org/10.1163/_q3_SIM_00374

Kuga, Y., Whitt, M. W., McDonald, K. C., & Ulaby, F. T. (1990). Scattering models for distributed targets. In *Radar polarimetry for geoscience applications*. Dedham, MA: Artech House. https://doi.org/10.1080/10106049009354274

Lee, J. S., & Pottier, E. (2009). *Polarimetric Radar Imaging*. *CRC Press*. https://doi.org/10.1201/9781420054989

Lesiv, M., See, L., Laso Bayas, J., Sturn, T., Schepaschenko, D., Karner, M., … Fritz, S. (2018). Characterizing the Spatial and Temporal Availability of Very High Resolution Satellite Imagery in Google Earth and Microsoft Bing Maps as a Source of Reference Data. *Land*, *7*(4), 118. https://doi.org/10.3390/land7040118

Li, X., Yeh, A., Liu, K., & Wang, S. (2006). Inventory of mangrove wetlands in the Pearl River Estuary of China using remote sensing. *Journal of Geographical Sciences*, *16*(2), 155–164. https://doi.org/10.1007/s11442-006-0203-2

Li, Z., Wright, T., Hooper, A., Crippa, P., Gonzalez, P., Walters, R., … Parsons, B. (2016). Towards InSAR everywhere, all the time, with Sentinel-1. *International Archives of the Photogrammetry, Remote Sensing and Spatial Information Sciences - ISPRS Archives*, *41*(July), 763–766. https://doi.org/10.5194/isprsarchives-XLI-B4-763-2016

Lück-Vogel, M., Mbolambi, C., Rautenbach, K., Adams, J., & Van Niekerk, L. (2016). Vegetation mapping in the St Lucia estuary using very high-resolution multispectral

imagery and LiDAR. https://doi.org/10.1016/j.sajb.2016.04.010

Mahdavi, S., Salehi, B., Granger, J., Amani, M., Brisco, B., & Huang, W. (2018). Remote sensing for wetland classification: a comprehensive review. *GIScience and Remote Sensing*, *55*(5), 623–658. https://doi.org/10.1080/15481603.2017.1419602

Mahdianpari, M., Salehi, B., Mohammadimanesh, F., Homayouni, S., & Gill, E. (2018). The First Wetland Inventory Map of Newfoundland at a Spatial Resolution of 10 m Using Sentinel-1 and Sentinel-2 Data on the Google Earth Engine Cloud Computing Platform. *Remote Sensing*, *11*(1), 43. https://doi.org/10.3390/rs11010043

Mahdianpari, M., Salehi, B., Mohammadimanesh, F., & Motagh, M. (2017). Random forest wetland classification using ALOS-2 L-band, RADARSAT-2 C-band, and TerraSAR-X imagery. *ISPRS Journal of Photogrammetry and Remote Sensing*, *130*, 13–31. https://doi.org/10.1016/j.isprsjprs.2017.05.010

Martinez, J. M., & Le Toan, T. (2007). Mapping of flood dynamics and spatial distribution of vegetation in the Amazon floodplain using multitemporal SAR data. *Remote Sensing of Environment*, *108*(3), 209–223. https://doi.org/10.1016/j.rse.2006.11.012

Maseko, M. S. T., Ramesh, T., Kalle, R., & Downs, C. T. (2017). Response of Crested Guinea-fowl (Guttera edouardi), a forest specialist, to spatial variation in land use in iSimangaliso Wetland Park, South Africa. *Journal of Ornithology*. https://doi.org/10.1007/s10336-016-1406-7

McFeeters, S. K. (1996). The use of the Normalized Difference Water Index (NDWI) in the delineation of open water features. *International Journal of Remote Sensing*. https://doi.org/10.1080/01431169608948714

Microsoft Bing Maps. (2018). Bing Maps. Microsoft.

Millennium Ecosystem Assessment. (2005). *Ecosystems and human well-being: wetlands and water*. Washington DC.

Mitsch, W. J., & Gosselink, J. G. (2006). *Wetlands*. *Program*. https://doi.org/10.1017/CBO9781107415324.004

Mleczko, M., & Mróz, M. (2018). Wetland mapping using SAR data from the Sentinel-1A and TanDEM-X missions: A comparative study in the Biebrza Floodplain (Poland). *Remote Sensing*, *10*(1). https://doi.org/10.3390/rs10010078

Moser, L., Schmitt, A., Wendleder, A., & Roth, A. (2016). Monitoring of the Lac Bam wetland extent using dual-polarized X-band SAR data. *Remote Sensing*, *8*(4). https://doi.org/10.3390/rs8040302

Mróz, M., Mleczko, M., & Fitrzyk, M. (2016). Exploitation of Sentinel-1a data in one year survey of water transfer on wetlands. *European Space Agency, (Special Publication) ESA SP*, *SP-740*(May).

Muro, J., Canty, M., Conradsen, K., Hüttich, C., Nielsen, A. A., Skriver, H., … Menz, G. (2016). Short-term change detection in wetlands using Sentinel-1 time series. *Remote Sensing*, *8*(10), 1–14. https://doi.org/10.3390/rs8100795

National Geospatial Information (South Africa). (2018). Aerial Photography.

National Wetlands Working Group. (1997). *The Canadian Wetland Classification System, 2nd edition*. Waterloo, Ontario.

Nicodemus, K. K. (2011). Letter to the editor: on the stability and ranking of predictors from random forest variable importance measures. *Briefings in Bioinformatics*. https://doi.org/10.1093/bib/bbr016

Novresiandi, D. A., & Nagasawa, R. (2015). Tropical peatland identification using L-Band full polarimetric alos PALSAR: A case study in Central Kalimantan, Indonesia. In *ACRS 2015 - 36th Asian Conference on Remote Sensing: Fostering Resilient Growth in Asia, Proceedings*.

Oshiro, T. M., Perez, P. S., & Baranauskas, J. A. (2012). How many trees in a random forest? In *Lecture Notes in Computer Science (including subseries Lecture Notes in Artificial Intelligence and Lecture Notes in Bioinformatics)*. https://doi.org/10.1007/978-3-642-31537-4_13

Ozesmi, S. L., & Bauer, M. E. (2002). Satellite remote sensing of wetlands. *Wetlands Ecology and Management*, *10*(5), 381–402. https://doi.org/10.1023/A:1020908432489

Pekel, J.-F., Cottam, A., Gorelick, N., & Belward, A. S. (2016). High-resolution mapping of global surface water and its long-term changes. *Nature*. https://doi.org/10.1038/nature20584

Planet. (2018). Image courtesy of Planet Labs, Inc. Retrieved October 31, 2018, from https://www.planet.com/explorer

QGIS Development Team. (2018). QGIS Geographic Information System. Open Source Geospatial Foundation Project. Retrieved from http://qgis.osgeo.org

R Core Team. (2018). R: A language and environment for statistical computing. Vienna, Austria: R Foundation for Statistical Computing. Retrieved from https://www.r-project.org/

Ramsar Secretariat. (2009). *Information Sheet On Ramsar Wetlands*.

Ramsar Secretariat. (2016). *The 4th Strategic Plan 2016 – 2024*.

Ramsar Secretariat. (2018). *Scaling up wetland conservation, wise use and restoration to achieve the Sustainable Development Goals "Wetlands and the SDGs."* Retrieved from https://medwet.org/publications/wetlands-and-the-sdgs/

Richards, J. A., Woodgate, P. W., & Skidmore, A. K. (1987). An explanation of enhanced radar backscattering from flooded forests. *International Journal of Remote Sensing*. https://doi.org/10.1080/01431168708954756

Rodriguez-Galiano, V. F., Ghimire, B., Rogan, J., Chica-Olmo, M., & Rigol-Sanchez, J. P. (2012). An assessment of the effectiveness of a random forest classifier for land-cover classification. *ISPRS Journal of Photogrammetry and Remote Sensing*, *67*(1), 93–104. https://doi.org/10.1016/j.isprsjprs.2011.11.002

Rosenqvist, A., Finlayson, C. M., Lowry, J., & Douglas, T. (2007). The potential of long-wavelength satellite-borne radar to support implementation of the Ramsar Wetlands

Convention. *Aquatic Conserv: Mar. Freshw. Ecosyst.*, *17*, 229–244.

Rosenqvist, Å., Forsberg, B. R., Pimentel, T., Rauste, Y. A., & Richey, J. E. (2002). The use of spaceborne radar data to model inundation patterns and trace gas emissions in the central Amazon floodplain. *International Journal of Remote Sensing*, *23*(7), 1303–1328. https://doi.org/10.1080/01431160110092911

Rutherford, M. C., Mucina, L., & Powrie, L. W. (2007). Vegetation Map of South Africa, Lesotho and Swaziland. *South African National Biodiversity Institute*.

Schlaffer, S., Chini, M., Dettmering, D., & Wagner, W. (2016). Mapping wetlands in Zambia using seasonal backscatter signatures derived from ENVISAT ASAR time series. *Remote Sensing*, *8*(5), 1–24. https://doi.org/10.3390/rs8050402

Semeniuk, V., & Semeniuk, C. A. (1997). A geomorphic approach to global classification for natural inland wetlands and rationalization of the system used by the Ramsar Convention - A discussion. *Wetlands Ecology and Management*. https://doi.org/10.1023/A:1008207726826

Shimada, M., Itoh, T., Motooka, T., Watanabe, M., Shiraishi, T., Thapa, R., & Lucas, R. (2014). New global forest/non-forest maps from ALOS PALSAR data (2007-2010). *Remote Sensing of Environment*. https://doi.org/zhou10.1016/j.rse.2014.04.014

Strobl, C., Boulesteix, A. L., Kneib, T., Augustin, T., & Zeileis, A. (2008). Conditional variable importance for random forests. *BMC Bioinformatics*. https://doi.org/10.1186/1471-2105-9-307

Tian, H., Li, W., Wu, M., Huang, N., Li, G., Li, X., & Niu, Z. (2017). Dynamic monitoring of the largest freshwater lake in China using a new water index derived from high spatiotemporal resolution sentinel-1A data. *Remote Sensing*, *9*(6), 6–9. https://doi.org/10.3390/rs9060521

Tiner, R. W. (1999). *Wetland Indicators: A Guide to Wetland Identification, Delineation, Classifcation, and Mapping*. *Boca Raton: CRC Press LLC*. https://doi.org/10.1201/9781420048612.ch1

Tiner, R. W., Lang, M. W., & Klemas, V. V. (2015). *Remote sensing of wetlands: Applications and advances*. *Remote Sensing of Wetlands: Applications and Advances*. https://doi.org/10.1201/b18210

Townsend, P. A. (2002). Relationships between forest structure and the detection of flood inundation in forested wetlands using C-band SAR. *International Journal of Remote Sensing*, *23*(3), 443–460. https://doi.org/10.1080/01431160010014738

Töyrä, J., & Pietroniro, A. (2005). Towards operational monitoring of a northern wetland using geomatics-based techniques. *Remote Sensing of Environment*, *97*(2), 174–191. https://doi.org/10.1016/j.rse.2005.03.012

Töyrä, J., Pietroniro, A., Martz, L. W., & Prowse, T. D. (2002). A multi-sensor approach to wetland flood monitoring. *Hydrological Processes*, *16*(8), 1569–1581. https://doi.org/10.1002/hyp.1021

Tsendbazar, N. E., de Bruin, S., Mora, B., Schouten, L., & Herold, M. (2016). Comparative assessment of thematic accuracy of GLC maps for specific applications using existing

reference data. *International Journal of Applied Earth Observation and Geoinformation*, *44*, 124–135. https://doi.org/10.1016/j.jag.2015.08.009

Tsyganskaya, V., Martinis, S., Marzahn, P., & Ludwig, R. (2018). Detection of temporary flooded vegetation using Sentinel-1 time series data. *Remote Sensing*, *10*(8). https://doi.org/10.3390/rs10081286

Wang, Y., Hess, L. L., Filoso, S., & Melack, J. M. (1995). Understanding the radar backscattering from flooded and nonflooded Amazonian forests: Results from canopy backscatter modeling. *Remote Sensing of Environment*. https://doi.org/10.1016/0034-4257(95)00140-9

Ward, D. P., Petty, A., Setterfield, S. A., Douglas, M. M., Ferdinands, K., Hamilton, S. K., & Phinn, S. (2014). Floodplain inundation and vegetation dynamics in the Alligator Rivers region (Kakadu) of northern Australia assessed using optical and radar remote sensing. *Remote Sensing of Environment*. https://doi.org/10.1016/j.rse.2014.02.009

Whyte, A., Ferentinos, K. P., & Petropoulos, G. P. (2018). A new synergistic approach for monitoring wetlands using Sentinels -1 and 2 data with object-based machine learning algorithms. *Environmental Modelling and Software*, *104*, 40–54. https://doi.org/10.1016/j.envsoft.2018.01.023

Wright, C., & Gallant, A. (2007). Improved wetland remote sensing in Yellowstone National Park using classification trees to combine TM imagery and ancillary environmental data. *Remote Sensing of Environment*. https://doi.org/10.1016/j.rse.2006.10.019

Wurm, M., Taubenböck, H., Weigand, M., & Schmitt, A. (2017). Slum mapping in polarimetric SAR data using spatial features. *Remote Sensing of Environment*, *194*, 190–204. https://doi.org/10.1016/j.rse.2017.03.030

Xing, L., Tang, X., Wang, H., Fan, W., & Wang, G. (2018). Monitoring monthly surface water dynamics of Dongting Lake using Sentinal-1 data at 10 m. *PeerJ*, *6*, e4992. https://doi.org/10.7717/peerj.4992

Xu, H. (2006). Modification of normalised difference water index (NDWI) to enhance open water features in remotely sensed imagery. *International Journal of Remote Sensing*. https://doi.org/10.1080/01431160600589179

Zhou, T., Li, Z., & Pan, J. (2018). Multi-feature classification of multi-sensor satellite imagery based on dual-polarimetric Sentinel-1A, Landsat-8 OLI, and hyperion images for urban land-cover classification. *Sensors*, *18*(2), 1–20. https://doi.org/10.3390/s18020373

8 Appendices

Appendix 1 – Sentinel-1 Image

Median composite RGB image of Sentinel-1 data in the study area.

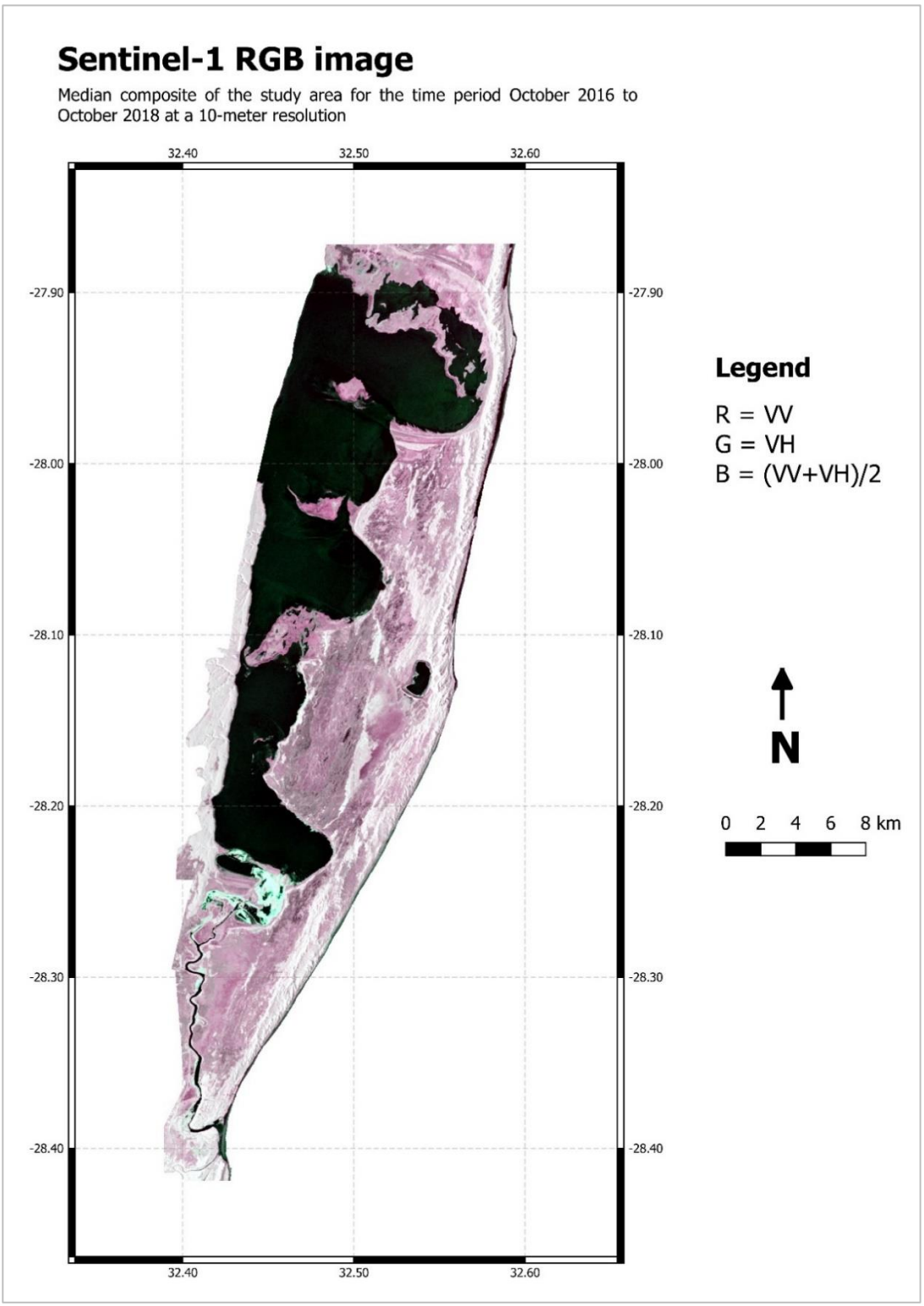

Appendix 2 – Sentinel-2 Image

Median composite RGB image of Sentinel-2 data in the study area.

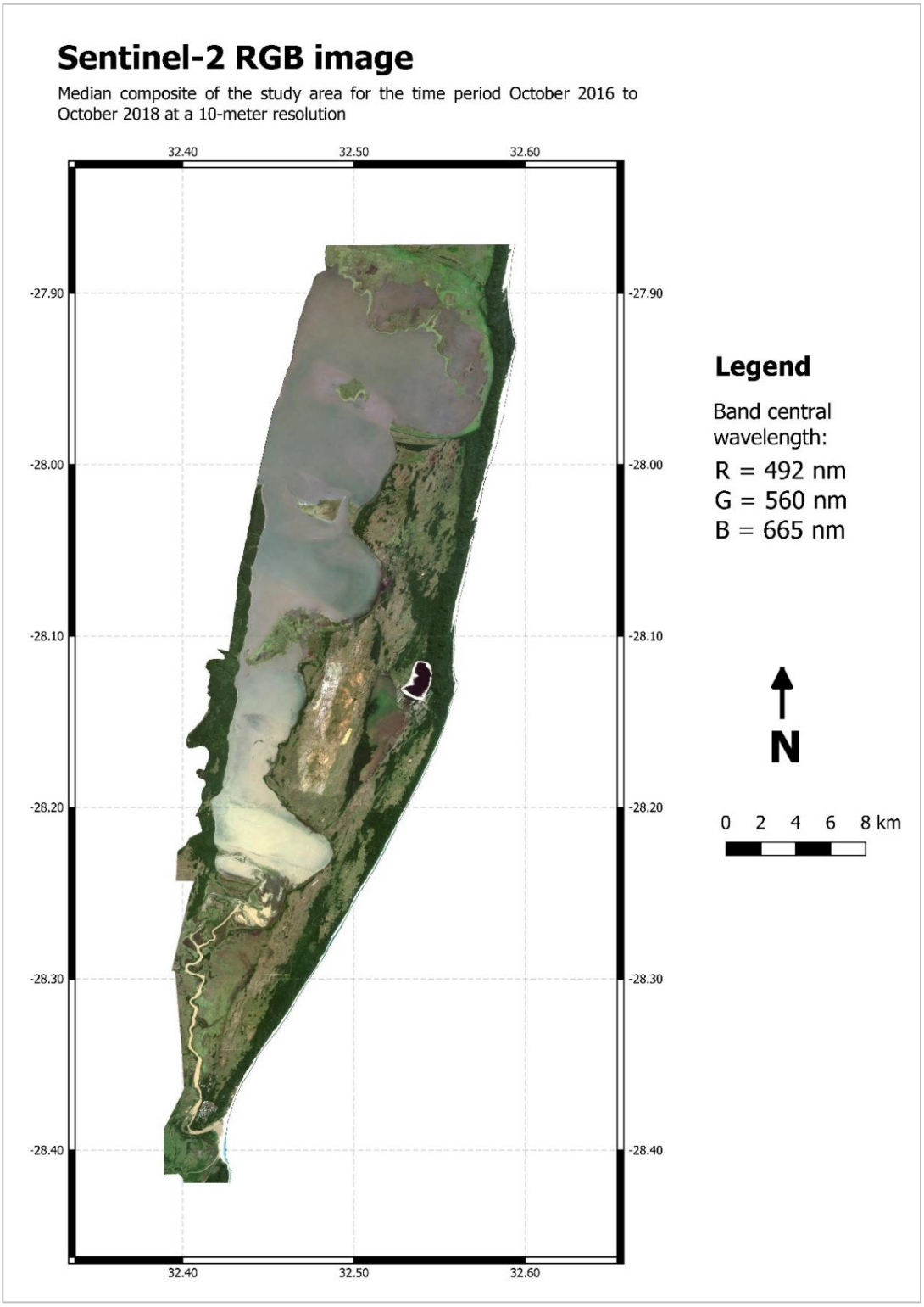

Appendix 3 – S1L1

Classification mode map

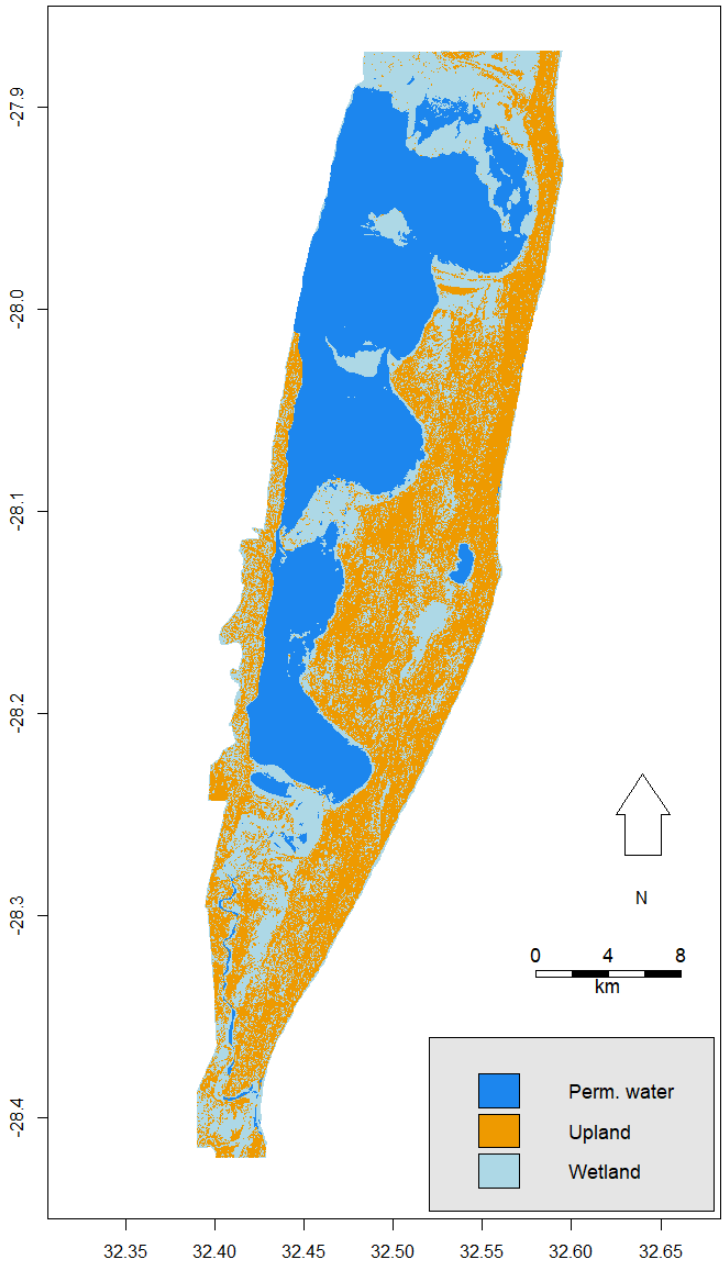

Mode frequency map

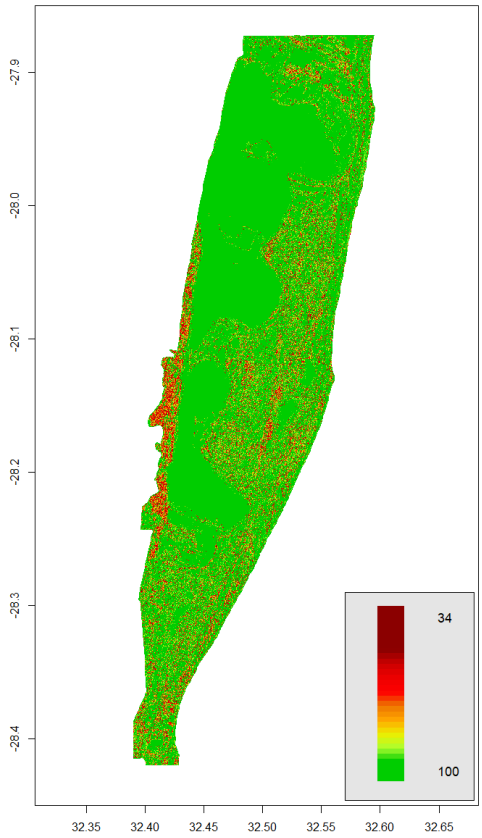

Mean variable importance

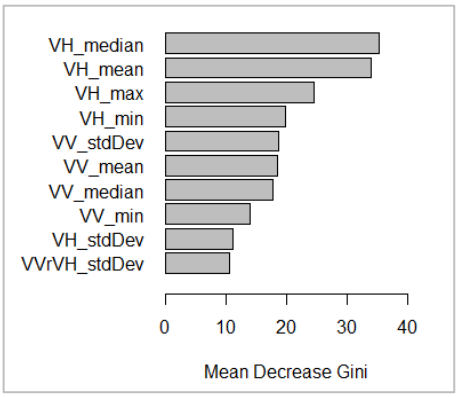

Confusion matrix and mean mode frequency

		Reference data				
		Pmt. water	*Upland*	*Wetland*	UA	MMF
Classification	*Pmt. water*	5960	36	89	97.9%	99.6
	Upland	40	4885	1286	78.7%	93.8
	Wetland	0	1079	4625	81.1%	92.6
	PA	99.3%	81.4%	77.1%	**85.9%**	

Appendix 4 – S1S2L1

Classification mode map

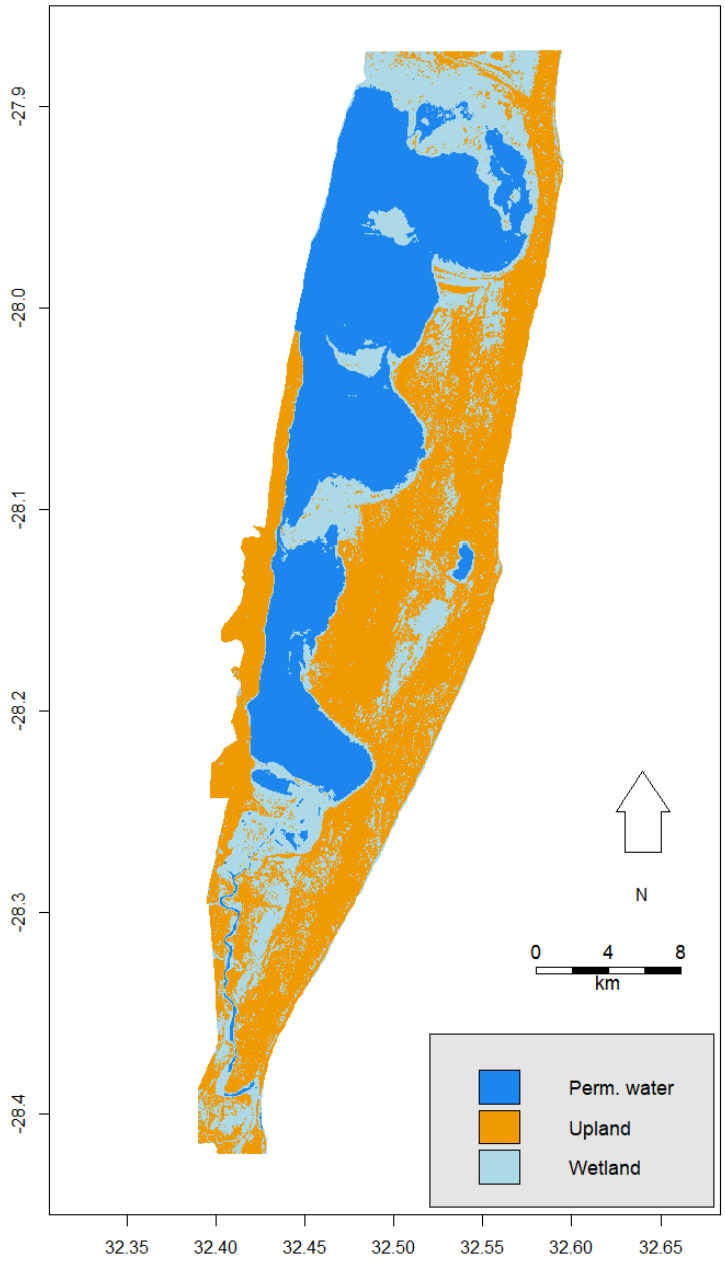

Mode frequency map

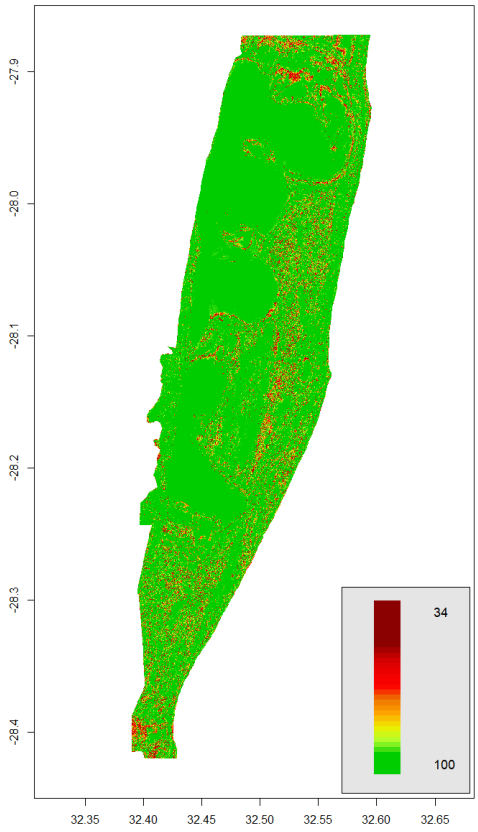

Mean variable importance

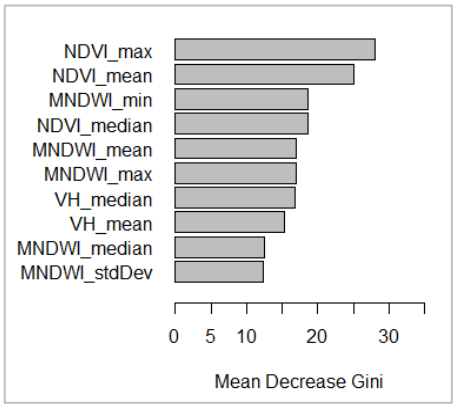

Confusion matrix and mean mode frequency

		Reference Data				
		Pmt. water	*Upland*	*Wetland*	UA	MMF
Classification	*Pmt. water*	6000	0	24	99.6%	99.4
	Upland	0	5602	897	86.2%	96.0
	Wetland	0	398	5079	92.7%	93.9
	PA	100.0%	93.4%	84.7%	**92.7%**	

Appendix 5 – S1L1$_{-HV}$

Classification mode map

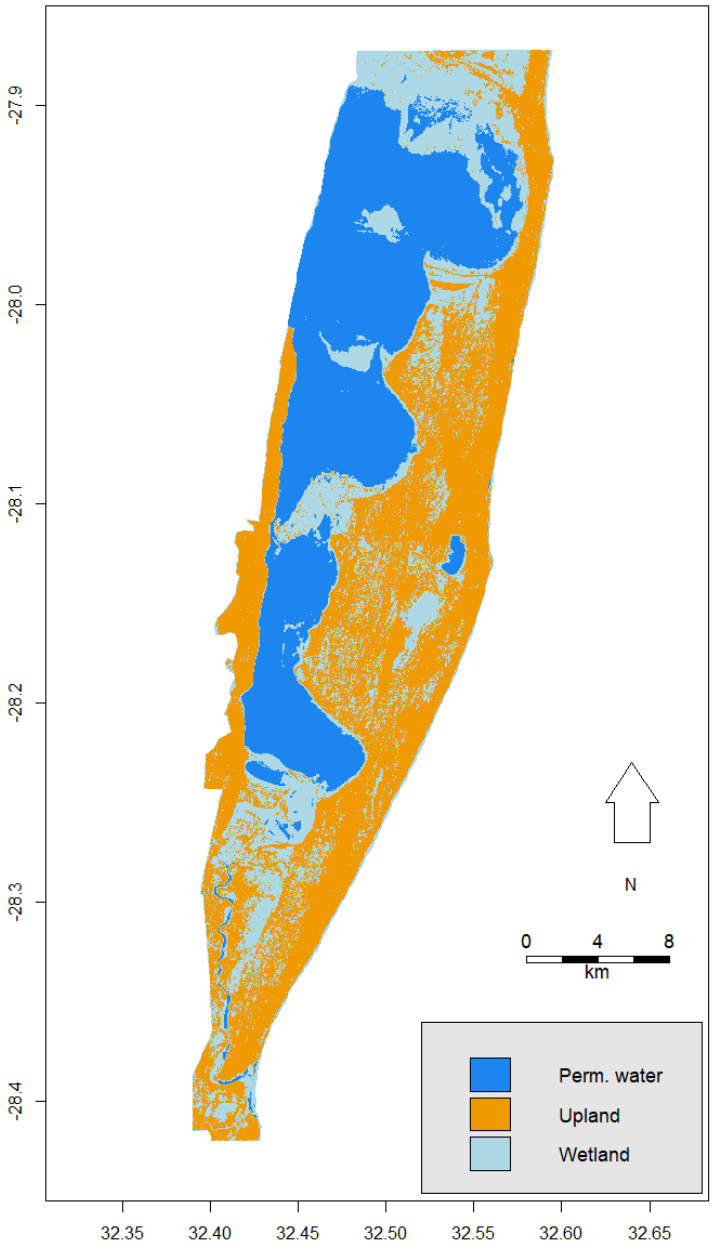

Mode frequency map

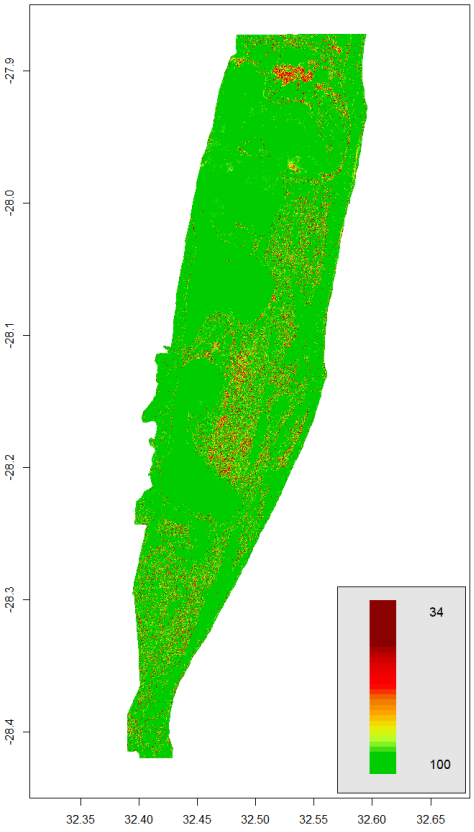

Mean variable importance

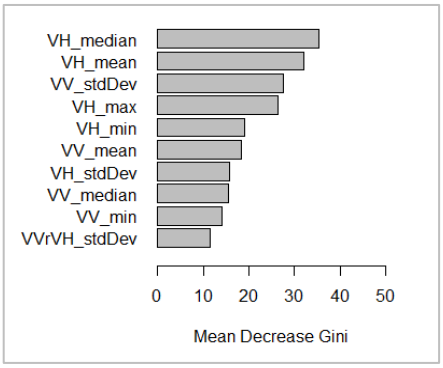

Confusion matrix and mean mode frequency

		Reference Data				
		Pmt. water	*Upland*	*Wetland*	UA	MMF
Classification	*Pmt. water*	5963	24	88	98.2%	99.4
	Upland	26	5545	496	91.4%	96.9
	Wetland	11	431	5416	92.5%	95.2
	PA	99.4%	92.4%	90.3%	**94.0%**	

Appendix 6 – S1S2L1$_{\text{-HV}}$

Classification mode map

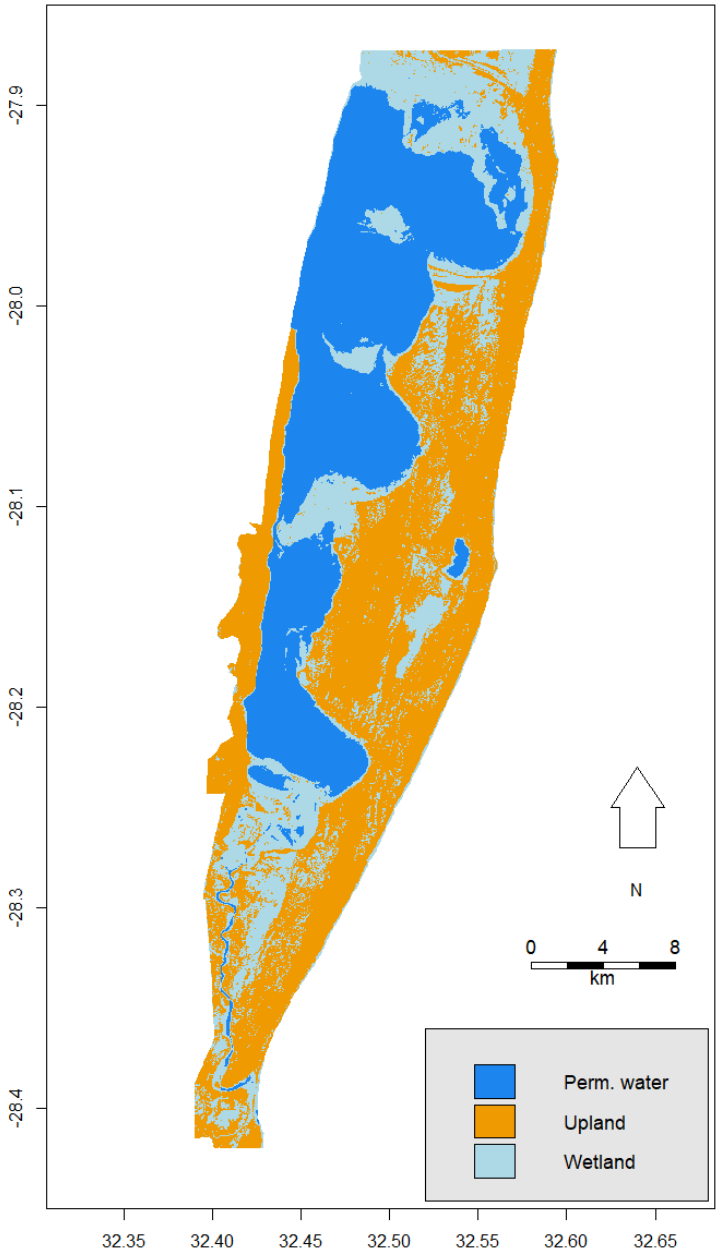

Mode frequency map

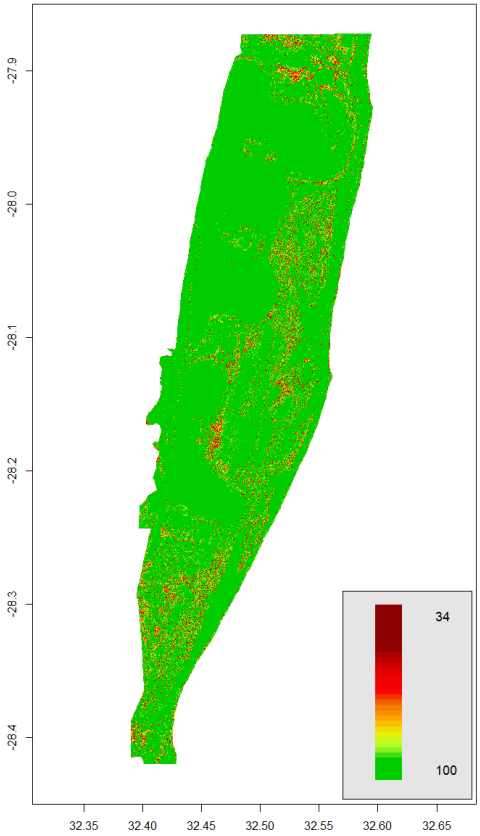

Mean variable importance

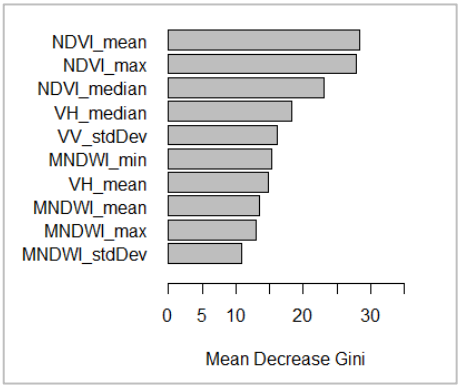

Confusion matrix and mean mode frequency

		Reference Data				
		Pmt. water	*Upland*	*Wetland*	UA	MMF
Classification	*Pmt. water*	6000	0	21	99.7%	99.5
	Upland	0	5876	390	93.8%	97.0
	Wetland	0	124	5589	97.8%	95.3
	PA	100.0%	97.9%	93.2%	**97.0%**	

Appendix 7 – S1L2

Classification mode map

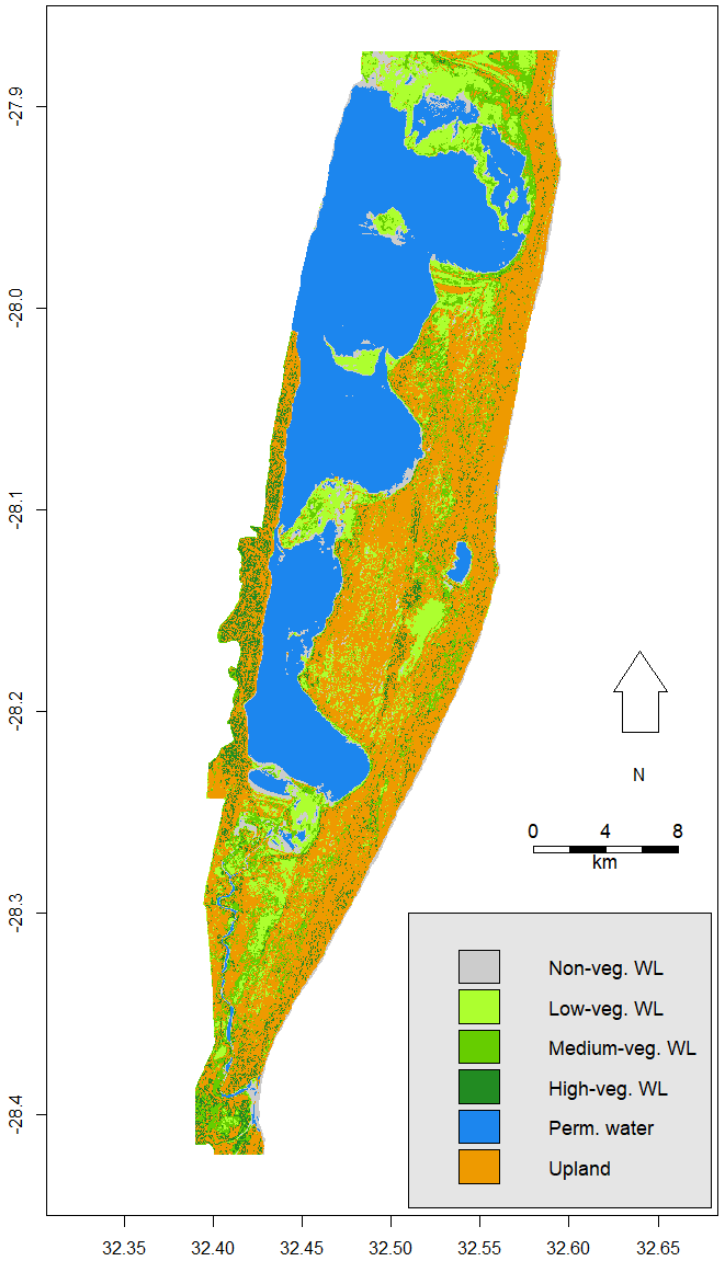

Mode frequency map

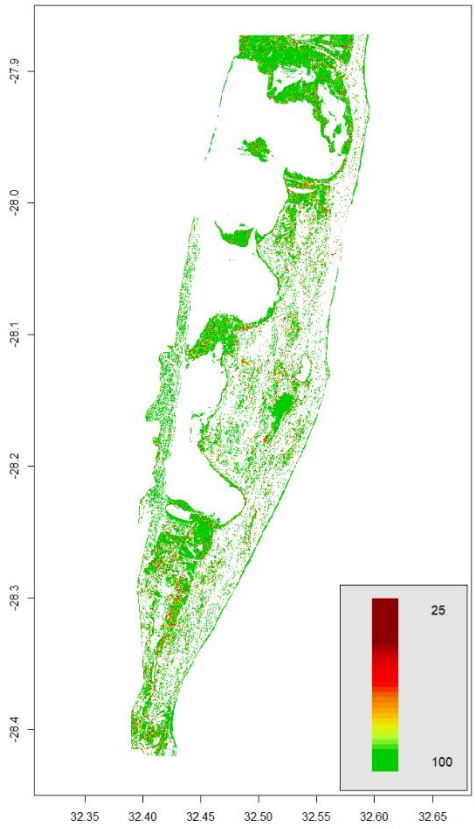

Mean variable importance

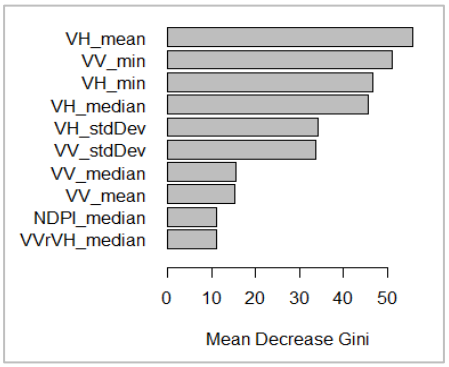

Confusion matrix and mean mode frequency

		Reference data				
		Non-veg.	*Low-veg.*	*Med.-veg.*	*High-veg.*	UA
Classification	*Non-veg.*	5950	53	44	0	98.4%
	Low-veg.	50	5537	778	4	86.9%
	Med.-veg.	0	410	4554	661	81.0%
	High-veg.	0	0	624	5335	89.5%
	PA	99.2%	92.3%	75.9%	88.9%	**89.1%**

MMF
98.0
95.6
92.8
95.7

Appendix 8 – S1S2L2

Classification mode map

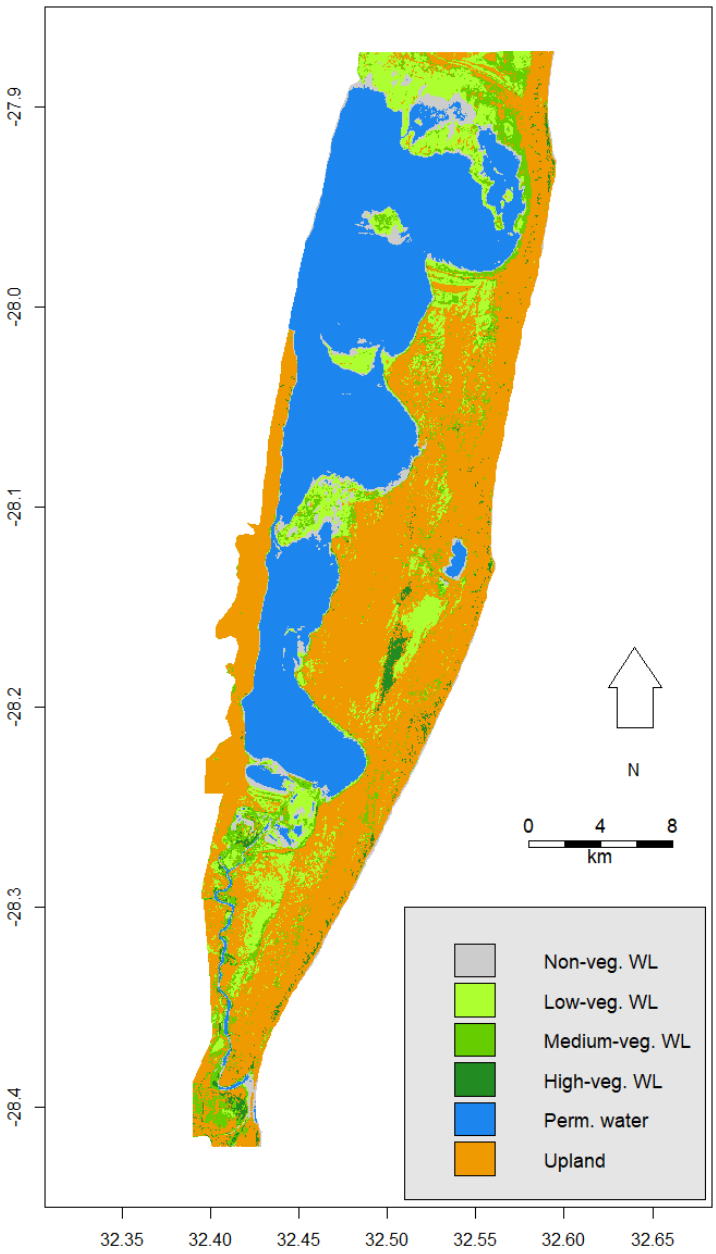

Mode frequency map

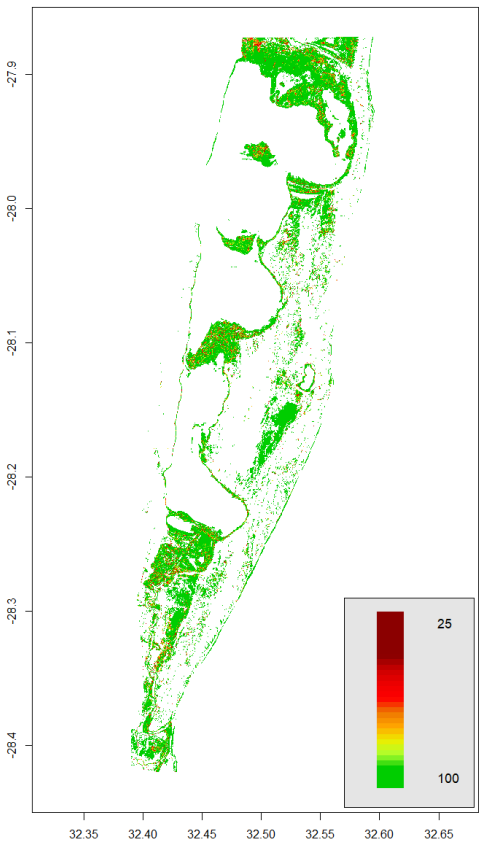

Mean variable importance

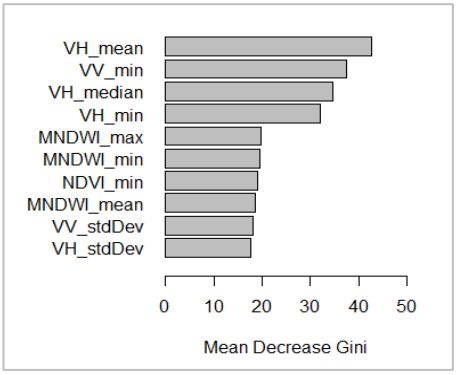

Confusion matrix and mean mode frequency

		Reference Data					
		Non-veg.	*Low-veg.*	*Med.-veg.*	*High-veg.*	UA	MMF
Classification	*Non-veg.*	5973	29	61	0	98.5%	98.8
	Low-veg.	27	5779	342	0	94.0%	96.2
	Med.-veg.	0	192	5322	476	88.8%	94.2
	High-veg.	0	0	275	5524	95.3%	96.5
	PA	99.6%	96.3%	88.7%	92.1%	**94.2%**	

Appendix 9 – S1L2$_{-HV}$

Classification mode map

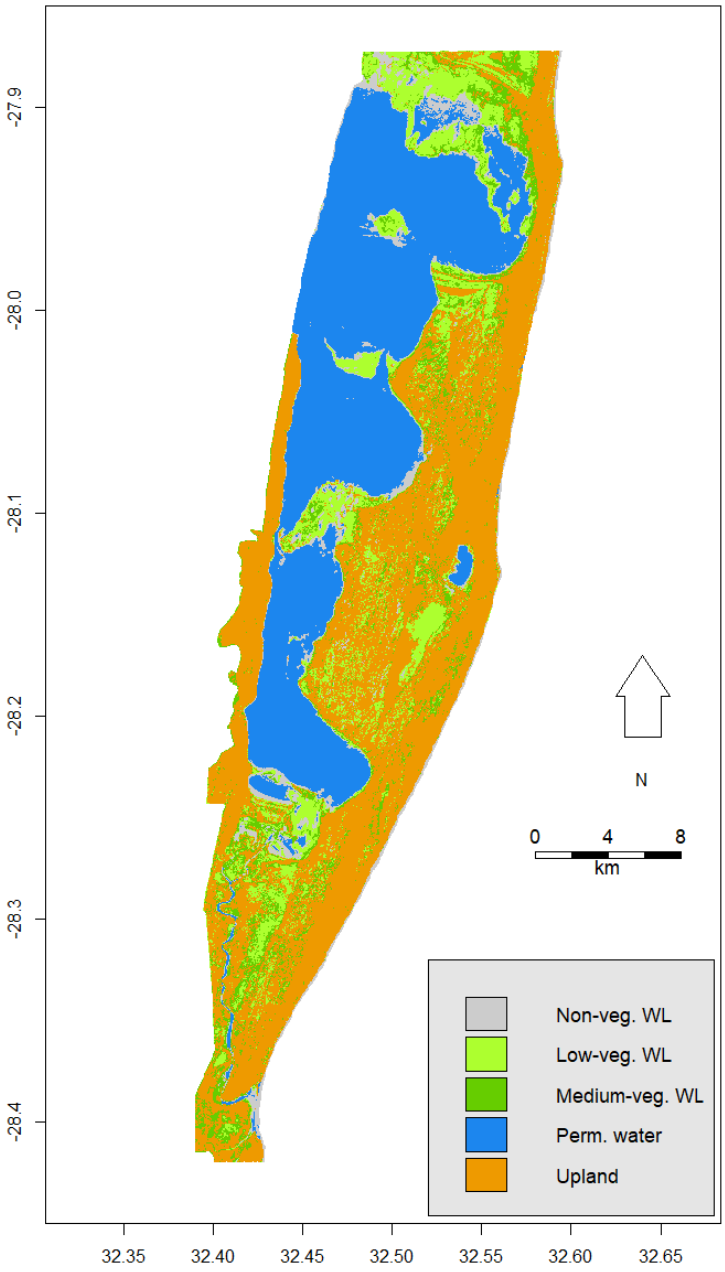

Mode frequency map

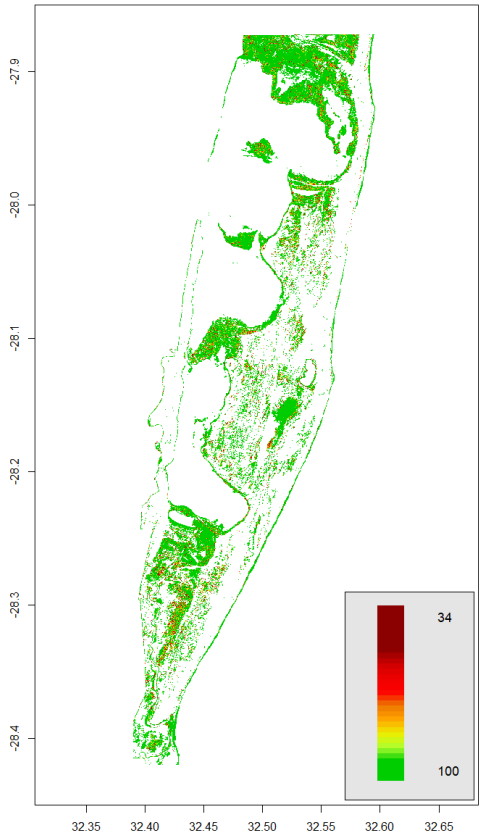

Mean variable importance

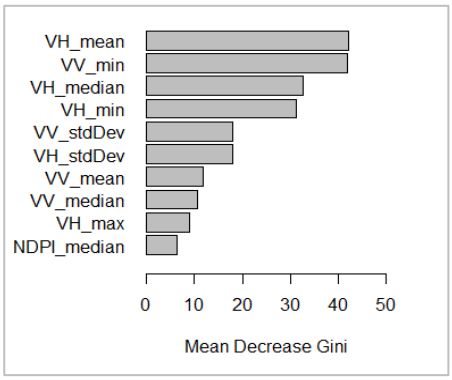

Confusion matrix and mean mode frequency

Classification	Reference Data				MMF
	Non-veg.	*Low-veg*	*Med.-veg.*	UA	
Non-veg.	5958	45	42	98.6%	98.2
Low-veg.	42	5486	809	86.6%	95.5
Med.-veg.	0	469	5149	91.7%	94.9
PA	99.3%	91.4%	85.8%	**92.2%**	

Appendix 10 – S1S2L2$_{\text{-HV}}$

Classification mode map

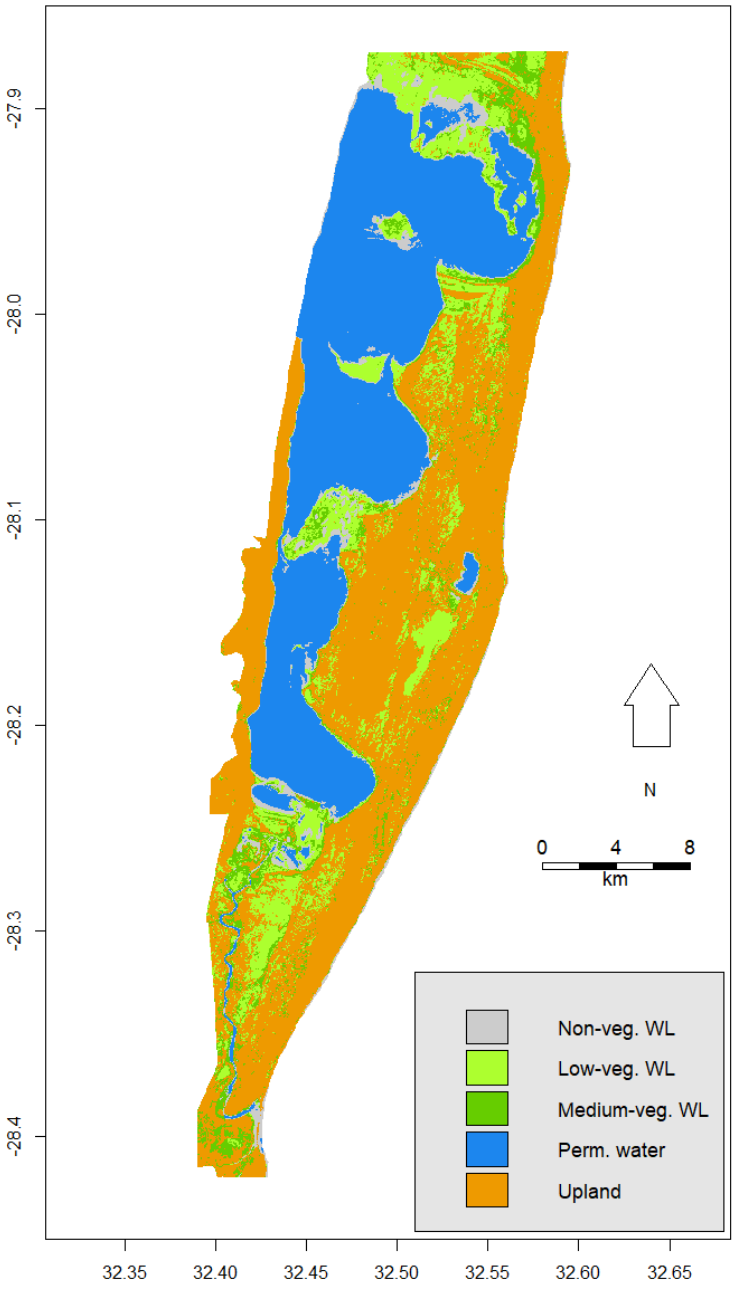

Mode frequency map

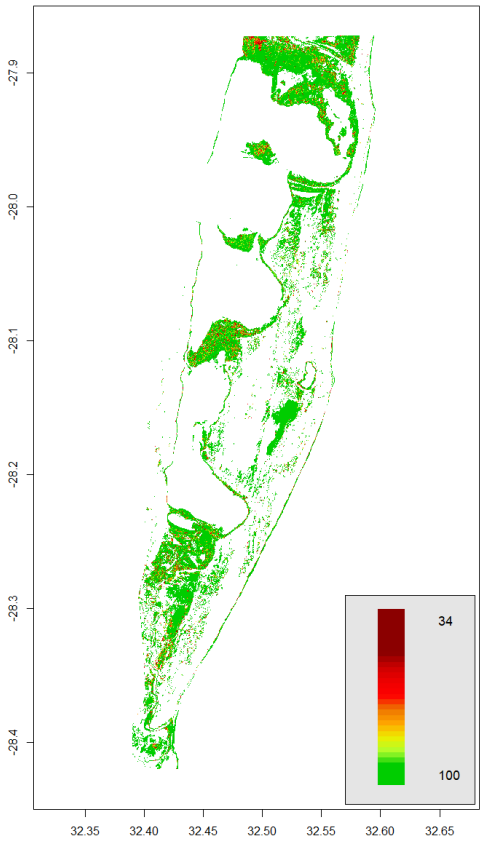

Mean variable importance

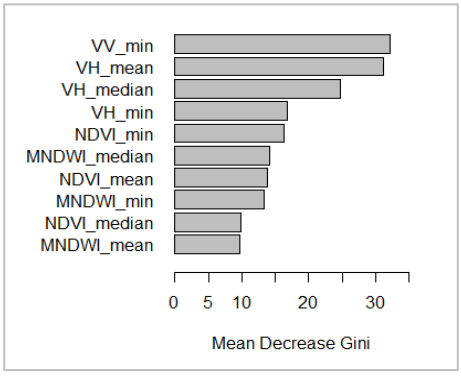

Confusion matrix and mean mode frequency

		Reference Data				
		Non-veg.	*Low-veg.*	*Med.-veg.*	UA	MMF
Classification	*Non-veg.*	5971	38	67	98.3%	98.5
	Low-veg.	29	5769	361	93.7%	96.5
	Med.-veg.	0	193	5572	96.7%	94.7
	PA	99.5%	96.2%	92.9%	**96.2%**	

Appendix 11 – S1L3

Classification mode map

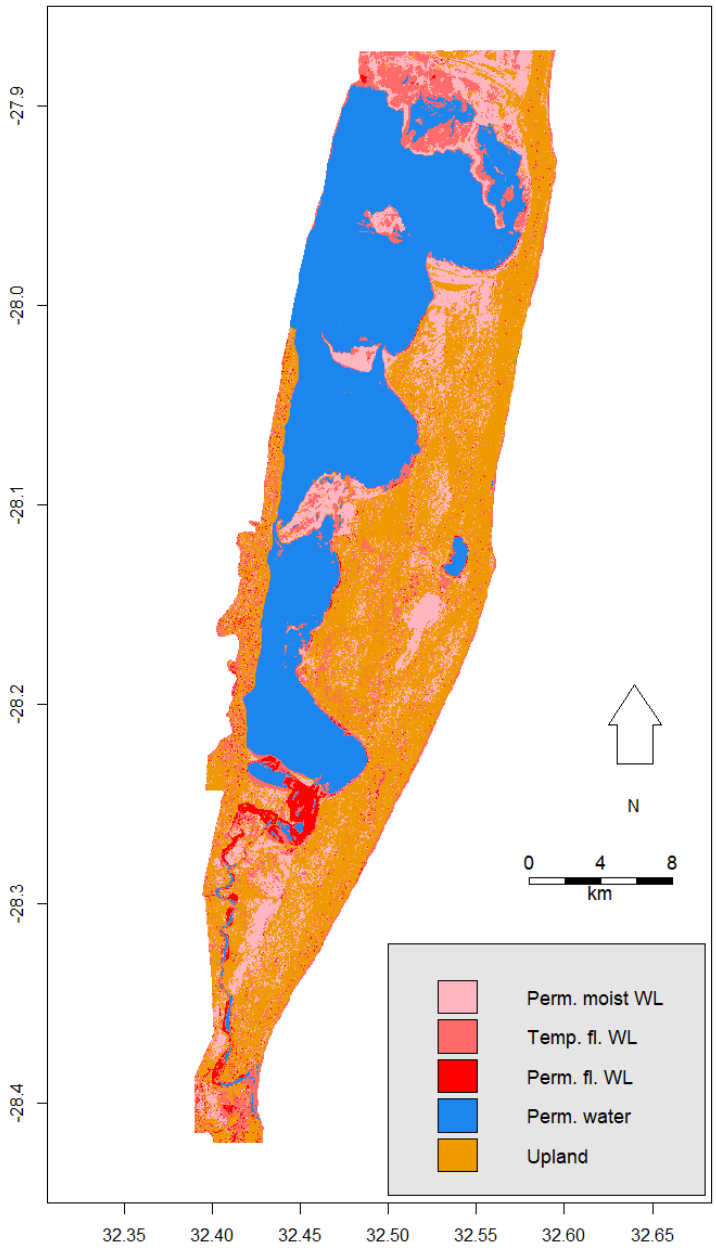

Mode frequency map

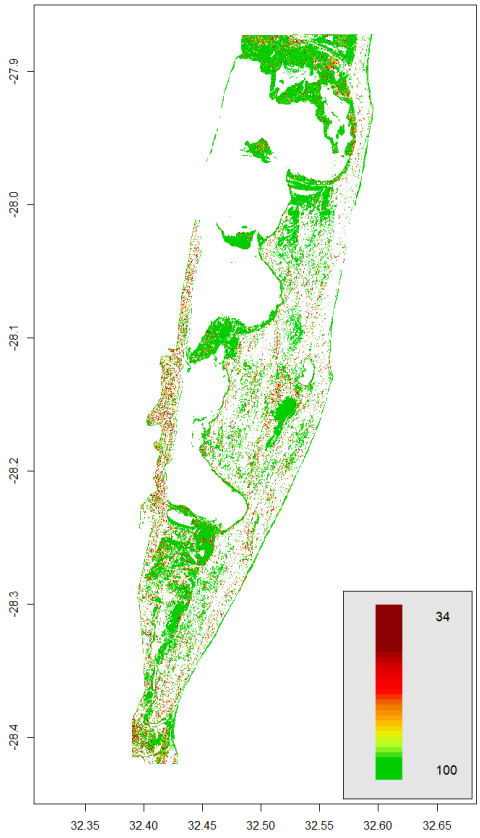

Mean variable importance

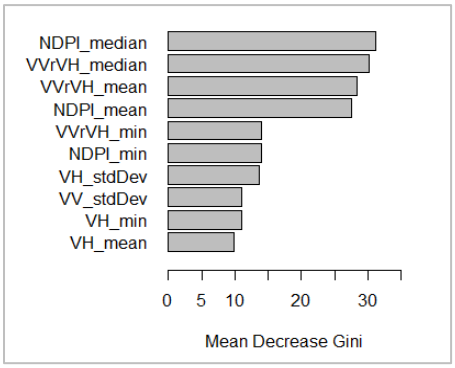

Confusion matrix and mean mode frequency

Classification	Reference Data				
	Pmt. moist	*Temp. fl.*	*Pmt. fl.*	UA.	MMF
Pmt. moist	5205	632	181	86.5%	95.3
Temp. fl.	710	4953	702	77.8%	92.4
Pmt. fl.	85	415	5117	91.1%	88.4
PA	86.8%	82.5%	85.3%	**84.9%**	

Appendix 12 – S1S2L3

Classification mode map

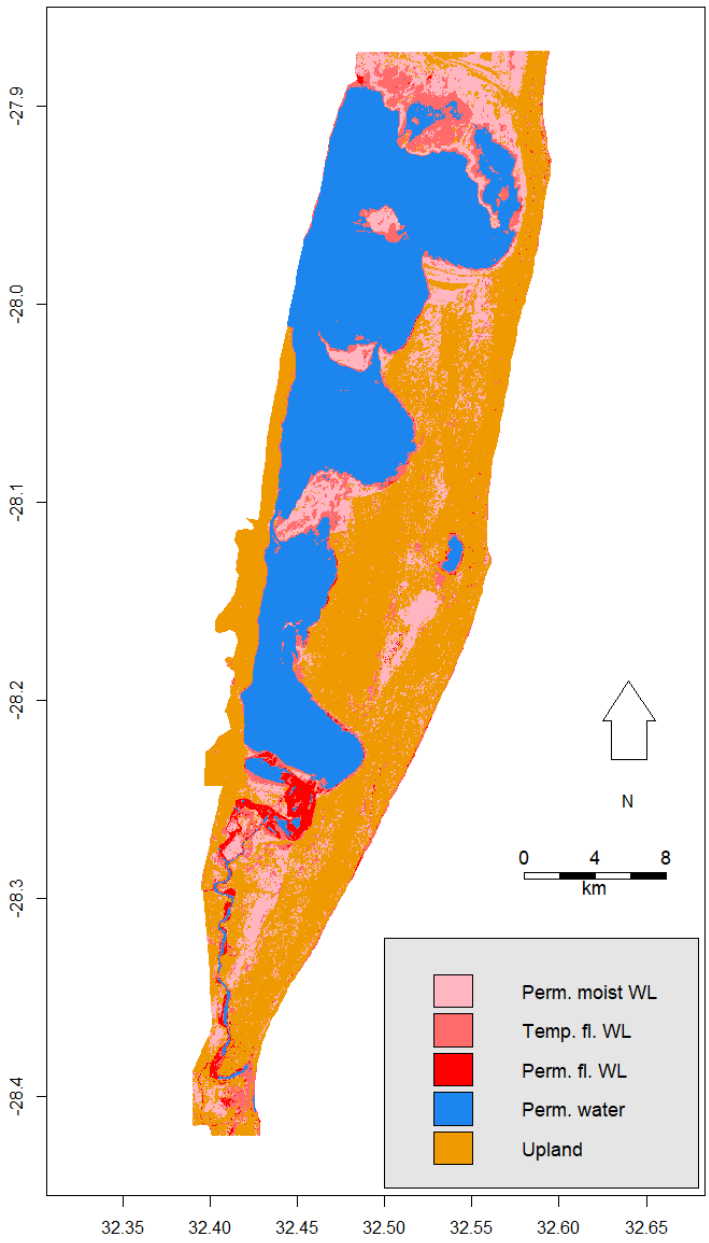

Mode frequency map

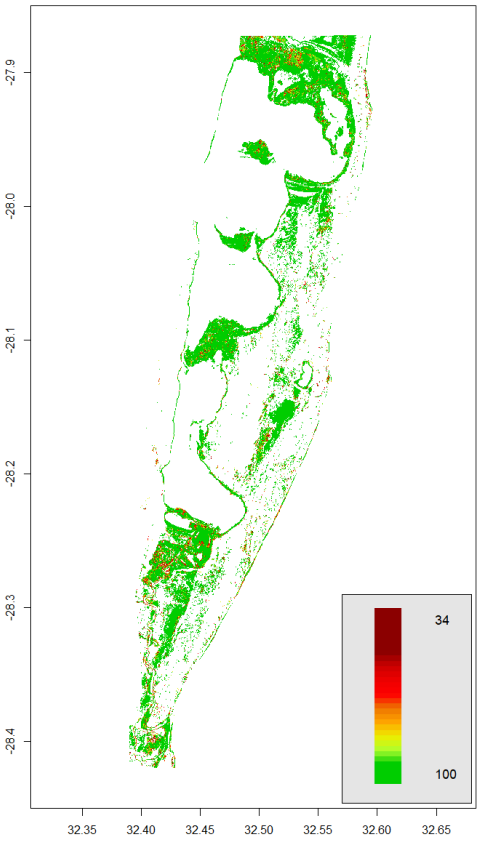

Mean variable importance

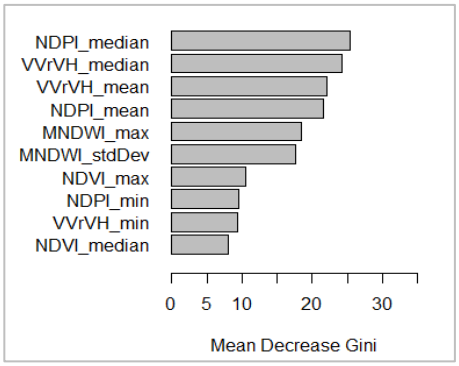

Confusion matrix and mean mode frequency

		Reference Data				
		Pmt. moist	*Temp. fl.*	*Pmt. fl.*	UA	MMF
Classification	*Pmt. moist*	5759	335	96	93.0%	97.5
	Temp. fl.	222	5353	512	87.9%	95.2
	Pmt. fl.	19	312	5392	94.2%	93.9
	PA	96.0%	89.2%	89.9%	**91.7%**	

Appendix 13 – S1L3$_{-HV}$

Classification mode map

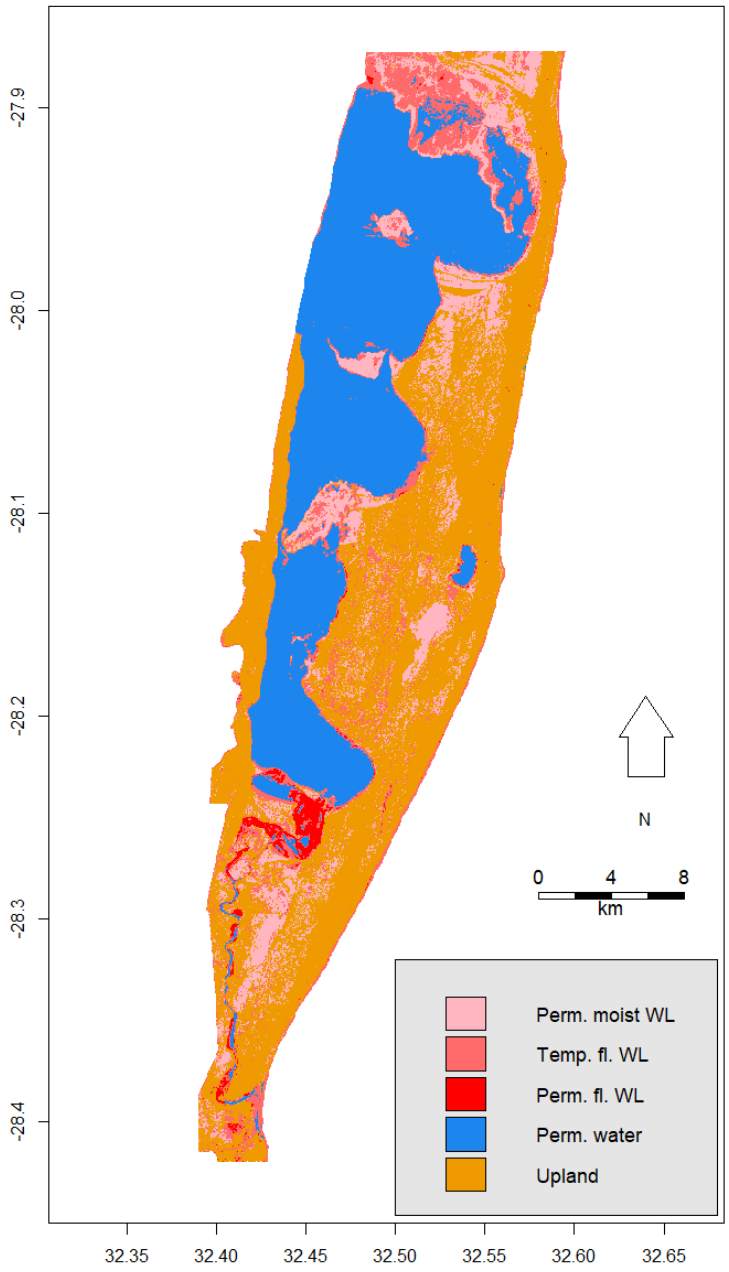

Mode frequency map

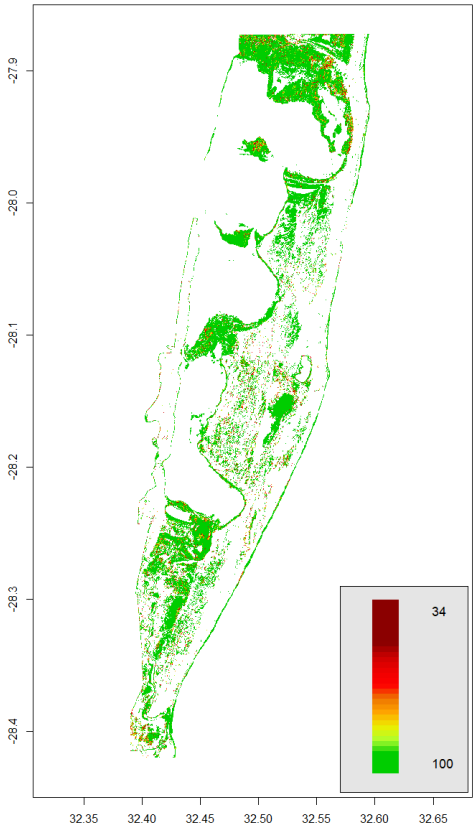

Mean variable importance

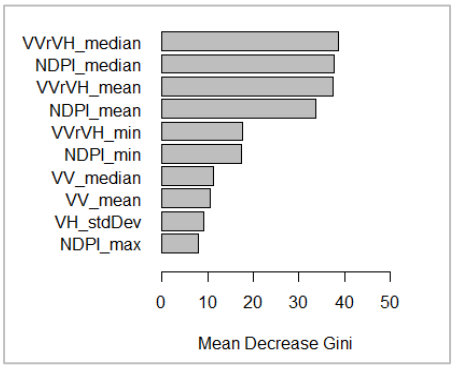

Confusion matrix and mean mode frequency

		Reference Data				
		Pmt. water	*Upland*	*Wetland*	UA	MMF
Classification	*Pmt. water*	6000	0	24	99.6%	99.4
	Upland	0	5602	897	86.2%	96.0
	Wetland	0	398	5079	92.7%	93.9
	PA	100.0%	93.4%	84.7%	**92.7%**	

Appendix 14 – S1S2L3$_{-HV}$

Classification mode map

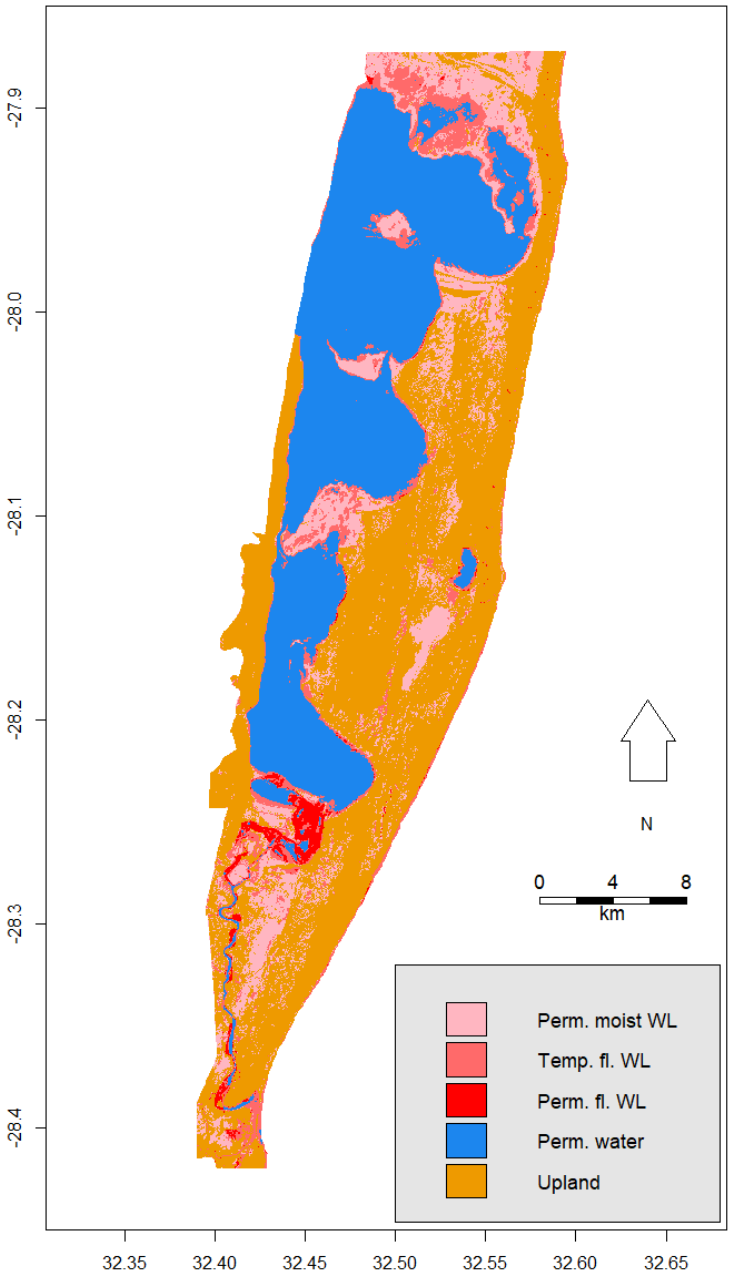

Mode frequency map

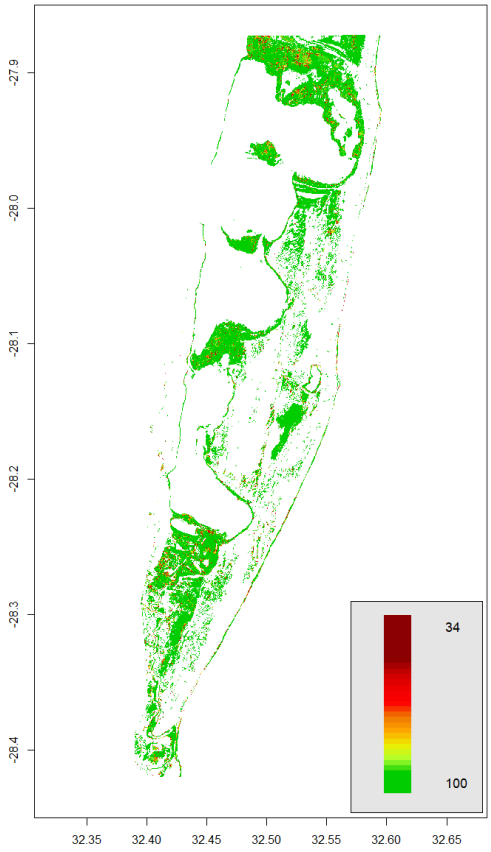

Mean variable importance

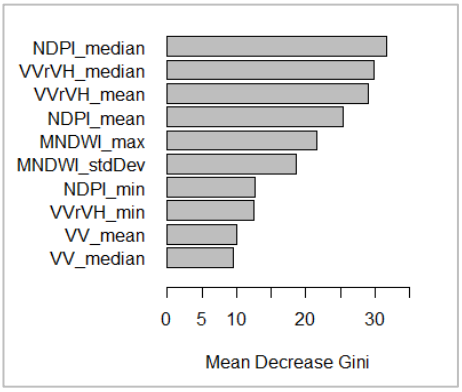

Confusion matrix and mean mode frequency

		Reference Data				
		Pmt. moist	*Temp. fl.*	*Pmt. fl.*	UA	MMF
Classification	*Pmt. moist*	5791	307	18	94.7%	97.9
	Temp. fl.	209	5558	95	94.8%	96.1
	Pmt. fl.	0	135	5887	97.8%	97.0
	PA	96.5%	92.6%	98.1%	**95.8%**	